

Editor Response

We greatly appreciate the opportunity to submit a revised manuscript. The reviewers shared many serious concerns about the content and presentation of our first submission, and we have made our strongest effort to address those concerns as thoroughly as possible. To that end, we have completely reworked this manuscript at every stage. We have isolated our data analysis to our own TA dataset from the Strait of Georgia, including new, previously unpublished profiles from our ongoing sampling program, and the Fraser River Water Quality Buoy pH record maintained by Environment and Climate Change Canada. Using only these data, we have produced a new suite of scenarios and executed new model runs to account for these changes. We have produced entirely new figures that clarify our model runs and our key points. Finally, we have rewritten the majority of our manuscript, particularly the results, discussion, and conclusions, to more clearly articulate our findings and emphasize our key points. We no longer attempt to extrapolate our results to other estuaries and instead only place our results in global contexts that are already well-established from existing literature. We feel that the revision process has strengthened this manuscript immensely, and we are grateful to the reviewers for their time and detailed comments.

Reviewer 1 Response

(*Reviewer Comments*, Response, Proposed Changes, **Added Changes**)

1. *This paper deals with the effect of variable boundary conditions in a river on the estuarine pH and saturation state. It does so by applying a previously described model that is used to run a large number of scenarios of feasible riverine conditions. Obviously the subject is an important one, and the tools used, modeling, are suitable to achieve the goals in the manuscript. However, I found this paper particularly difficult to read and to keep focus on the findings that it describes. In the end I even wonder what it is that I have learned here that I did not already know ... while the subject is an important one, the way the manuscript is structured does not lead to a large enough increase in insight for this paper to be accepted in its current state.*

We appreciate the detailed feedback provided by yourself, the other reviewer and the editor, and would enjoy the opportunity to revise the manuscript in accordance. We agree that we have extended some of our analyses beyond their scope and in doing so have unwittingly lost focus in the manuscript. We propose that we scale back to focus our analyses only on the Fraser River. We will still place it in the context of other global rivers (Figure 6) however we will remove the end-member analysis that relied on DIC and TA from other world rivers (Figures 5-d and 7).

Specifically, we will provide additional detail concerning the Fraser and its estuary, including what is known and less known regarding the drivers of the inorganic carbon cycle. The river is a key driver and yet we have few reliable carbon data in the fresh and brackish waters in the study region. This paucity provides a strong motivation for our analysis. By clarifying this motivation in the text, the key results will be highlighted. We will include the additional references (not all of which were available at the time that this manuscript was submitted) that the reviewers have suggested, where appropriate. We also will define new sensitivity scenarios to include more recent and newly acquired data where possible and reduce (and sometimes remove) the dependence on data in which we have less confidence (such as data collected using outdated methods or river TA with high organic alkalinity uncertainty). We will re-run all the simulations with these new scenarios and produce a new sensitivity summary figure (4), with clarified presentation, to reflect these new results. Finally, we will strengthen the delivery of our main findings and highlight the importance of using the biogeochemical coupled model by refocusing our results (3), discussion (4), and conclusion (5) sections to target the key points below.

Key points

- (a) Responses of estuarine pH and Ω_A to Fraser River DIC-TA are asynchronous and strongest at opposite ends of the Fraser DIC:TA range.
- (b) Seasonal estuarine productivity reduces estuarine pH sensitivity to river chemistry during summer
- (c) Future Fraser River flow regimes with lower flow in the biologically productive season will favor lower estuarine pH and Ω_A , but the river will dominate a smaller areal region in the estuary.

- We have removed the endmember discussion for other world estuaries beginning on page 14, line 15 and ending on page 15 line 8.
- We have added additional background about the study area starting on page 3: line 32
- We have addressed additional references in the introduction on page 2: lines 9, 11, 16, 17, 20, 28, and 29, and in the discussion on page 16: lines 5 and 33
- We have completely reworked the analysis beginning with new data and analysis (Figs. 2 and S1, Table 2), new model runs and analysis (Figs. 3–7) and strengthened presentation throughout.
- We have clarified our main findings and made them consistent throughout the manuscript in abstract (page 1, lines: 11-19), introduction (page 3: lines 11-14), results (page 11: lines 17-25), discussion (page 12: lines 30-35, page 13: lines 1-12, page 16, lines: 24-34) and conclusions (lines 17-32)

2. ... *figure 4 is particularly difficult to interpret. A few well-chosen scenarios would have been much easier to explain and to depict.*

Figure 4 depicts our key results (which will be clarified/focused) from the model sensitivity study, and is critical to the paper. We have constructed new scenarios based on current (rather than old/suspect) data. We plan to improve the accessibility of this figure by strengthening its description in the text (Section 3.2), and by making the following modifications

- The new scenarios will simply be numbered, with a table of associated freshwater pH, TA, DIC:TA, and DIC-TA values. We will plot the box and whisker objects against these scenario numbers in order of increasing freshwater TA or DIC:TA
- We will add a figure that shows a few selected years as timeseries plots and explain how these timeseries map to points on Figure 4 to clarify where this synopsis figure comes from.
- We will overplot selected individual years of salinity (a), DIC:TA (b, c), pH (d, e), and aragonite undersaturation duration (f, g) on top of the salinity climatology (a) and box statistics (b-g). These individual years will illustrate how each year fits into the box plot.
- We have created a new summary figure (Fig. 6) based on new scenarios and model runs. We now plot each model run individually and clearly distinguish it from the other runs using color, and exploring two selected runs (2010 and 2012) for additional scrutiny.
- We have added 3 new figures leading up to our main summary figure (Fig. 6) including a timeseries figure (Fig. 4) of selected model runs to illustrate the temporal behavior of the model before proceeding to the salinity averages. The runs from the timeseries plots are clearly indicated on Fig. 6 (stars)

- We have moved the salinity panel to its own plot with the river hydrograph also shown (Fig. 3). Again we have plotted the individual years as traces instead of the envelope around the mean curve.
- We have completely reworked our discussion of these plots, taking the time to carefully explain each one while remaining clear and concise

3. *... too little information is given about the system under study, so that it is not clear what processes might actually produce the patterns or how relevant these findings are for other systems.*

We wrote our study area section (2.1) with the intention of introducing the relevant processes in the Fraser-Strait of Georgia system for later discussion, but we now agree with the reviewers that the level of background presented and the degree to which that background is addressed in the discussion are inadequate. Specifically, it is important for the reader to recognize that the Fraser is globally significant (largest Pacific-draining river in Canada) and strongly seasonal, yet confined to a long residence time in the estuarine Strait of Georgia by tides and topography, the results of which are strong seasonal stratification, productivity, and near-surface aragonite undersaturation in the Strait. These processes are all resolved or parameterized in the model and present fundamental differences between the modelling results in Section 3.2 and the endmember mixing exercise in Section 4.1. Furthermore, these processes are not equally important in all estuaries and thus provide indicators for the applicability of this study to other systems. In the new manuscript, we will refocus Section 2.1 so that it supports the narrative that we have described here.

We have added additional information about the study area to highlight the importance of the river and biology in determining the existing carbonate chemistry of the system starting at Page 3: line 33.

4. *it is even unclear if the 1-D model resolves the vertical extent (which I think it does) or has the dimension arranged along the estuarine length axis (which I think it should).*

The model is 1-D vertical. This vertical model was used rather than an estuarine length axis model because local phytoplankton seasonality is more sensitive to the wind and light climatology than to the river (but the river is still important). The vertical mixing model resolves these wind (stratification within a deep fjordic system) and light effects on phytoplankton mechanistically. In contrast, a (1-D) horizontal model would have to parameterize these effects. We will add more details of the model configuration including the above motivation. Also we will highlight the uniqueness of our vertical formulation, specifically how it accounts for estuarine circulation (originally only cited - Collins et al 2009.)

We have clarified this point beginning on page 4: line 22

5. *The 2008 paper from Salisbury et al, that is used to back up the scarcity of papers on estuarine carbonate chemistry is outdated by 10 years, and there are indeed some recent papers on this subject that are not mentioned in the manuscript, e.g., Volta et al., 2015 (Hydrol. Earth Sys. Sci.), Cai et al., 2017 (Nat. Comm.) to name a few. There is also older work e.g., Regnier et al., 1997 (Mar Chem.)*

Agreed. We have thoroughly reviewed these suggested studies and will integrate them into the Introduction and Discussion sections of this manuscript.

We have addressed additional references in the introduction on page 2: lines 9, 11, 16, 17, 20, 28, and 29, and in the discussion on page 16: lines 5 and 33

6. *while the paper shows that, under some conditions of freshwater influence, the estuarine pH and [aragonite] saturation appears more sensitive, it is not clear why this is so ... procedures to formalize the attribution of processes on pH shifts have been ... recently put in a consistent framework by Hagens and Middelburg, 2016 (Geochim. Cosmochim. Acta)*

We did explore the use of sensitivity (or buffer) factors - e.g., Egleston et al., 2010 (GBC), Soetaert et al., 2007 (Mar. Chem.) - particularly in discussing our sensitivity results along the salinity gradient - e.g., Hu and Cai, 2013 (GRL). Ultimately we decided against using these sensitivity factors since we were trying to communicate the effects of *freshwater* chemistry on properties within a dynamic and productive estuary, which in the endmember mixing case (Section 4.1) are simply caused by the surplus (or deficit) of DIC at the freshwater endmember being mixed into the estuarine zone. We realize that this endmember behavior alone is not new research, but our intention was to put our model sensitivity results in the context of simple mixing. We believe that the endmember mixing analysis supports these results and helps to highlight the important effects of our model sources and sinks within the estuary. We will clarify our intention for the endmember analysis in Section 4.1 and include a brief discussion of why we used that analysis rather than sensitivity factors.

We have clarified the mechanisms influencing the strength of sensitivity in our model on page 12: lines 23-29. Since changes in the freshwater endmember are affecting conditions in the estuary and buffer factors would describe a change in estuarine sensitivity at given estuarine changes, we opted not to use a buffer factor analysis.

Reviewer 2 Response

(*Reviewer Comments*, Response, Proposed Changes, **Added Changes**)

1. *I must admit that I am conflicted in making a recommendation of this paper. First, this is my favorite subject and I like the approach of a combination of data and modeling (also a combination of numerical model and simple mixing model). However I do not think the combination is successful ... If the authors can address these serious issues reasonably, I feel this paper can be a good contribution to our field. Here are my suggestions ... if the numerical model study of the Fraser case is new (say it), perhaps expand the model description and limit your discussion to this case, which is essentially what you did but just don't call it global extrapolation.*

We appreciate the detailed feedback provided by yourself, the other reviewer and the editor, and would enjoy the opportunity to revise the manuscript in accordance. We agree that we have extended some of our analyses beyond their scope and in doing so have unwittingly lost focus in the manuscript. We propose that we scale back to focus our analyses only on the Fraser River. We will still place it in the context of other global rivers (Figure 6) however we will remove the end-member analysis that relied on DIC and TA from other world rivers (Figures 5-d and 7).

Specifically, we will provide additional detail concerning the Fraser and its estuary, including what is known and less known regarding the drivers of the inorganic carbon cycle. The river is a key driver and yet we have few reliable carbon data in the fresh and brackish waters in the study region. This paucity provides a strong motivation for our analysis. By clarifying this motivation in the text, the key results will be highlighted. We will include the additional references (not all of which were available at the time that this manuscript was submitted) that the reviewers have suggested, where appropriate. We also will define new sensitivity scenarios to include more recent and newly acquired data where possible and reduce (and sometimes remove) the dependence on data in which we have less confidence (such as data collected using outdated methods or river TA with high organic alkalinity uncertainty). We will re-run all the simulations with these new scenarios and produce a new sensitivity summary figure (4), with clarified presentation, to reflect these new results. Finally, we will strengthen the delivery of our main findings and highlight the importance of using the biogeochemical coupled model by refocusing our results (3), discussion (4), and conclusion (5) sections to target the key points below.

Key points

- (a) Responses of estuarine pH and Ω_A to Fraser River DIC-TA are asynchronous and strongest at opposite ends of the Fraser DIC:TA range.
- (b) Seasonal estuarine productivity reduces estuarine pH sensitivity to river chemistry during summer
- (c) Future Fraser River flow regimes with lower flow in the biologically productive season will favor lower estuarine pH and Ω_A , but the river will dominate a smaller areal region in the estuary.

- We have removed the endmember discussion for other world estuaries beginning on page 14, line 15 and ending on page 15 line 8.
- We have added additional background about the study area starting on page 3: line 32
- We have addressed additional references in the introduction on page 2: lines 9, 11, 16, 17, 20, 28, and 29, and in the discussion on page 16: lines 5 and 33
- We have completely reworked the analysis beginning with new data and analysis (Figs. 2 and S1, Table 2), new model runs and analysis (Figs. 3–7) and strengthened presentation throughout.
- We have clarified our main findings and made them consistent throughout the manuscript in abstract (page 1, lines: 11-19), introduction (page 3: lines 11-14), results (page 11: lines 17-25), discussion (page 12: lines 30-35, page 13: lines 1-12, page 16, lines: 24-34) and conclusions (lines 17-32)

2. ... *the paper doesn't present much new data. I believe most new data and the numerical model were published in their two earlier publications (authors really need to say what is new here).*

We appreciate reviewer 2's comment and will revise to clearly lay-out the novelty of this study. This study examines the response of near-surface DIC:TA, pH and aragonite saturation state in our 1-D model (presented originally in Moore-Maley 2016 - detailing model evaluation and basic results/drivers for a *single* river chemistry) across more than 200 year-long runs with different river chemistry scenarios. The results of these runs with varied river chemistry are not published elsewhere. (The run parameters were chosen to simulate our best understanding of seasonal Fraser River DIC and TA, based on previously published total alkalinity observations in and around the river delta, an unpublished mooring pH timeseries in the river delta and finally, limited data mostly with $S > 20$ from the Fraser estuary - which were published in Ianson et al. 2016.) We will add some more recent new unpublished data from the Fraser estuary (single campaigns in 2014, 2016 and 2017) to further inform new sensitivity scenarios. These data will be highlighted.

We will also shorten and de-emphasize the data methods section (2.2) and move our discussion of organic alkalinity to the study area description (2.1) to clarify that this is a modelling study. We will also scale back our data description in the last paragraph of the introduction to allow the modelling objectives stated there appear more clearly to the reader.

We have refocused our data analysis to only include estuarine samples for which we have confidence (Fig. 2). We have also condensed our data analysis and merged it with our description of the sensitivity analysis, which comes after the model description on starting on page 6: line 30. This change helps highlight that this is a modelling study.

3. ... *the first sentence in the beginning of the Discussion (p.8, line 18-20) says: "To conceptualize why model estuarine pH is lowest at high TA_f " ... this statement is only true in the situation the authors created that is the ratio of river DIC:TA*

= 1.02 to 1.1 ... it is not “high TA_f ” but a high (DIC-TA) or DIC:TA in river water that is important here and is the reason behind the phenomenon ... I refer the authors to the paper by Liang et al. 2017 ...

We agree with the interpretation of reviewer 2 here that the changes in the freshwater DIC-TA (at constant DIC:TA ratio) are responsible for the pH vs S differences between the low and high freshwater TA cases. We also acknowledge that we refer to freshwater TA changes throughout this manuscript without mentioning DIC, which is misleading since we are always in fact manipulating either freshwater DIC:TA or freshwater DIC-TA or both. We will clarify our discussion of river TA scenarios in terms of DIC:TA and DIC-TA.

We have clarified the roles of DIC:TA and DIC-TA which are discussed on page 12 beginning at line 25, also shown in Fig. 7d

4. *... in extrapolation of the results, the authors didn't consider temperature effect but this effect can also be significant in controlling carbonate system speciation.*

We plan to limit the generalization of our results in other estuaries and remove Figure 7 and the last 3 paragraphs of Section 4.2.

We have removed the discussion of endmembers in other estuaries

5. *If the examples cited by the authors are also true in the Fraser River (e.g., as high as 90% of TA is organic alk), then, how can we believe the DIC_f calculated from the pH_f and TA_f ?*

We based our freshwater TA endmembers on several data sources, some of which were collected in the Fraser River. By limiting our new endmember scenarios to data collected in the Strait of Georgia where we expect organic alkalinity contributions to be less significant, we can reduce the uncertainty in these scenarios. We will add more recent observations from the Strait of Georgia (see REVISION V above) and remove all TA data collected using outdated methods or in freshwater where organic alkalinity uncertainty is high.

We have scaled back our data analysis to only include estuarine data. We have mentioned the remaining uncertainty in our analysis on page 7 starting at line 19

6. *... the extrapolation of the Fraser River DIC:TA ratio globally is just not appropriate ... please fully assess the uncertainty of your assumptions. Here the assumption of $DIC_f:TA_f > 1.02$ probably not just changes the result slightly it perhaps will change the major conclusion derived.*

We have decided to remove the extrapolation to global rivers including the last figure. We will only put the Fraser River in *context* of global rivers (Figure 6 in the original manuscript).

We have removed this discussion from the manuscript.

7. *... the paper is poorly prepared and hard to follow (see my detailed reading notes) ... the writing is not transparent to me. So a thorough rewrite with a better readability is also needed.*

The paper will be thoroughly revised (see the “Outline” in our response to the Editor) and we will use your detailed reading notes.

We have thoroughly reworked this paper beginning from the data, construction of the scenarios, rerunning the model, remaking the figures and rewriting most sections particularly the results, discussion, and conclusions to more clearly guide the reader through our findings and weave our key points in throughout the manuscript.

8. *Fig. 4 is particularly hard to understand or guess.*

The revision will include an additional figure with selected (model) timeseries from individual years. We will explain how we go from the time series to points on Figure 4 to clarify where this synopsis figure comes from (see point IX in our response to Editor). We will also clarify the text.

We have completely reworked this figure and provided 3 new figures leading into it. We have replaced the envelope and box plots with individual points to show the reader exactly which model runs we are looking at. One of the new lead in plots shows the timeseries of selected runs, illustrating to the reader the seasonal patterns of the model over time so that the salinity averages are less ambiguous.

9. *... p.9, line 10, it says "This asynchrony arises because the response of estuarine carbonate ion over the large range of river TA_f and pH_f scenarios is more sensitive to changes in total DIC than shifts in the equilibrium point of the carbonate system." First, I don't understand what this sentence really says. Second, it sounds like to suggest that one can change all three parameters (TA_f , pH_f and DIC_f) at the same time. If here "DIC" is not river DIC but internal estuarine, biologically modified DIC, this is probably true, but the authors didnt say that.*

We will clarify this sentence. The first phrase is confusing. Briefly, we wish to indicate that the concentration of the carbonate ion is more sensitive to the total amount of DIC (in the estuary) than the balance between the forms of DIC (which varies with pH). Your next point builds on this result.

We have rewritten this idea into the new discussion starting on page 12: line 30. We have clearly written the word "estuarine" before any non river value, and subscript f where we refer to freshwater values.

10. *In the abstract (p.1, line 10), it says "rivers with high DIC and TA produce lower estuarine pH due to an increased estuarine DIC:TA ratio, but higher estuarine Ω_A because of DIC contributions to the carbonate ion." I like this statement. But I do not really see the result description and an extensive discussion of in the text body. Does this indicate that authors have changed mind a bit on exactly what they want to focus on in this this paper?*

Thank you. As explained above we will refocus the paper. The difference between the response of pH and Ω_A is a key point and will be a focus in the revision.

We have removed this statement and tried to state this concept in terms of the mechanisms controlling this behavior, see abstract page 1 lines 11-23, results page 11: lines 18-25, discussion beginning on page 12: line 30

11. *I do not like the implications for future climate. You have speculated too much! (To say high atmospheric CO_2 will increase river pCO_2 is simply wrong as river pCO_2*

is generally so much higher than the atm-pCO₂.) So simplify it and merge it in the Discussion with just a few sentences.

We will significantly rework our future climate implications section (again, please see the “Outline” in our response to Editor) so that it concerns only the Fraser river and clearly focuses on changes in the Fraser’s hydrograph (decreasing freshet) that are anticipated with higher certainty. Potential changes in end-member chemistry will be discussed briefly and with care, clearly detailing the high uncertainty.

Reviewer 2 points out correctly that our text was misleading, and that many rivers are not likely to have increased DIC in future. Some fresh water end-members however may have increased DIC, as they tend to be at atmospheric equilibrium (e.g. glacial melt-water). As reviewer 2 knows, future DIC extrapolations also depend on the concurrent T change (a T increase could leave DIC unchanged even with increased pCO₂) leaving significant unknowns and low certainty.

We have reworked this paragraph to only refer to the Fraser – Strait of Georgia system, and directly address our findings from the sensitivity study. We have also spoken more generally about rising CO₂ at either the freshwater or seawater endmember

12. *Finally your summary is too long and repeats too much of the Discussion.*

The summary will be focused on the key points list above and we will ensure it is not repetitive.

We have rewritten the conclusions to be more concise and tied more closely to our main points

13. *p.2, Line 15-16, Is this true? I have not seen a river whose TA is NOT flow-dependent. Perhaps, it is because the West paper is about the silicate weathering. Not sure if this is also true for carbonate weathering.*

We did not intend to indicate that TA in other rivers is not flow-dependent. Our intent was rather to divide strongly flow-dependent from weakly flow dependent. We will rewrite this paragraph for clarity.

We have removed this statement since we no longer focus on this type of flow dependence

14. *p.4, line 15-18, Carbonate Alk is about 50% in the Satilla River Georgia (Cai et al. 1998). Again Cai et al. (1998) paper should be cited as it is the first study of this issue.*

Noted. We will cite Cai et al. 1998 with respect to organic alkalinity in the new manuscript.

We have added a citation for this study on page 4: line 13

15. *p.4, Line 15-18, this really worries me. If TA data quality is so bad and the organic contribution is so large, how do we know the rest of modeling is correct?*

We will add more recent discrete observations from the Fraser estuary (point 5 above) and remove all TA data collected using outdated (and even uncertain) methods or in freshwater where organic alkalinity uncertainty is high.

We have limited our data analysis to estuarine TA data for which we have higher confidence. We continue to use the buoy pH record and acknowledge the remaining uncertainty in our TA extrapolations. We also continue to maintain that these data are simply for guiding our selection of model sensitivity experiments (page 7: lines 22-26). We have also moved our data discussion after the model methods and integrated into the sensitivity methods to further emphasize that the data are not the primary method of the study.

16. *p.6, Is RMSE = 0.16 pH unit a small uncertainty? It appears quite large to me. Perhaps you need to put it in the context of overall pH change.*

Good point. We will add the range of pH and also calculate a Willmott score to show the model skill.

Reviewer 2 is correct that variability in pH is indeed high in the estuary - the new figure with individual year timeseries traces will also add context for the reader.

We have rewritten the model evaluation section to give more detail about the model evaluation, clarifying that the large RMSE contains systematic bias, and the non-systematic RMSE is much lower. Given the systematic bias, the model is conservative and overpredicts pH and Omega. See page 6: lines 22-29

17. *p.7, line 11 says “We define our three constant TA_f scenarios”, then line 17 says “We define our three constant pH_f scenarios (Table 2)” (first there is no pH_f in Table 2). I am quite confused if these are related or separated assumptions? From my comment below on Fig. 5 caption, I don’t think you need to call them “constant TA_f or pH_f”, just river endmember scenario 1 to 6 is enough. They have nothing to do with whether TA_f is constant with river discharge; they are just your scenarios.*

We used a combination of scenarios: so 3 different pH_f and 6 different TA_f for a total of 18 different scenarios, hence 18 boxes on each plot in Table 4. We will completely restyle our presentation our analyses (see response to Editor - VIII) in terms of DIC/TA and DIC-TA and we will assign a run-number, as reviewer 2 suggests, to each model river chemistry scenario. Also, the scenarios themselves will be revised (Editor response – VII).

We have summarized our scenarios into Table 2 and refer to them consistently based on that table throughout. We have also improved the figure legends to reflect the layout of that table, especially Figs. 6 and 7. We also refer to the scenarios using consistent language, usually by the actual value (e.g., TA_f = 500 umol/kg), or in the case of DIC_f:TA_f, “Low, Med and High Carbon”

18. *p.7, line 20, I do not understand this: “Given the large seasonal temperature change (> 15 °C increase in summer), a constant pH_f implies a summer DIC_f decrease due to temperature (causing DIC_f:TA_f to decrease by about 0.06)”. Why does increased temperature lead to DIC_f decrease? Is this just a decreased solubility effect or increased river pCO₂ leads to more CO₂ degassing? Do you mean that under constant pH_f and Alk_f, higher temperature leads to lower DIC_f? That is true. But the real question is what is really controlling the pH_f at constant TA_f*

but allowing DIC_f to decrease? You can't just set a certain parameter constant arbitrarily. Anyway you need to explain your assumption. Reading Fig. 5 caption (b), I finally see how you did it. You selected two TA_f values one low and one medium-high. Then at each TA_f , you selected three pH_f values and calculated 6 DIC_f values. Then you take these 6 TA_f and DIC_f combinations and mix them with the same seawater (TA_{sw} and DIC_{sw}) to generate the 6 mixing lines. I assume at least b and c should be based on these 6 same simulation. (For panel d, it seems you used the variable TA_f .) My question is: are these combinations realistic? I now take your 6 combinations and put them into CO2SYS (I assume $T = 15^\circ C$ and all other acid = 0) and verified/confirmed your DIC_f and $DIC_f:TA_f$. No problem except that all $DIC_f:TA_f$ ratio > 1.02 . This doesn't make sense to me. Perhaps it is true for the low TA_f rivers (but in these river the org-ALK is often large), $DIC:TA < 1$ definitely occurs in medium and high TA rivers.

First, we are grateful to reviewer 2 for their meticulous consideration of our scenarios. Reviewer 2 is correct in that our intent was to indicate that "... at constant pH_f and Alk_f , higher temperature leads to lower DIC_f according to CO2SYS" however, it is clear that our original text was confusing. Our response above to #17 fully clarifies our previous scenarios and more importantly our plans to significantly revamp both the actual river chemistry scenarios and their presentation. (The mismatch in reviewer 2's CO2SYS results and our scenario is due to the fact that the actual T in the Fraser river and in our model is not static - varying from 4-20 °C during the year.)

We have changed our use of freshwater pH scenarios to using freshwater DIC:TA scenarios. We have also explicitly stated the values for several key carbonate system parameters in fresh water under each of these scenarios in Table 2.

19. *p.7, line 30-33, It is very hard to understand what the authors try to say after reading this part and Fig. 4 many times. Are DIC:TA (Fig. 4b) or pH (Fig. 4d) averaged over the estuary or what? Very frustrating.*

Again we thank reviewer 2 for their careful review. The revision will include an additional figure with example time series (Editor - IX and response to #8 above). We will explain how we go from the timeseries to points on Figure 4 to clarify where this synopsis figure comes from. The new discussion of the individual traces will clarify the averaging.

We have completely restructured the presentation of our results, including new figures to lead into the summary figure more gradually, especially Fig. 4 which show timeseries of selected model runs throughout the year. These runs then go on to appear on the summary figure highlighted as red and black stars. We have also included a paragraph in the results dedicated to explaining this figure carefully to the reader. Finally the figure itself is simpler. There are no boxes or salinity envelopes, just a single circle point per run, 216 points in total.

20. *p.8, the description of Fig. 4 is not very clear. Figure 4 is not clearly labeled. Some supplement instructions are needed. (Like does all gray and white sections in figure 4b, 4c, 4d mean different pH scenario? What does the "5 and 4" mean in figure 4f)?*

A new revision will include an additional figure with example time series. We will explain how we go from the time series to points on Figure 4 to clarify where this synopsis figure comes from. We will complete the labelling.

See our response to 19 above

21. *p.8, I am shocked that line 16 moves into Discussion. Now I realized that the entire ms is essentially a model study of pH sensitivity to river discharge and $(DIC:TA)_f$ ratio (the latter is also a function of discharge). Then, I went back to read their two earlier papers. The mode and the field data were already presented there. The authors need to say what is new of the first part of this paper comparing with the earlier papers.*

We see that our original submission failed to put this new work in the context of the original model paper. See our detailed response to #2. Again, our previous papers focused on the estuarine carbon cycle as forced by physical and biological conditions in the estuary. However during that research it became clear that the river chemistry also had a substantial impact. This manuscript looks at that impact. All the model runs are new, as river chemistry was not varied in the previous model paper. We have also collected new data which will be included in the new manuscript.

We have clarified the nature of this study in multiple places. It is probably best clarified in the model description starting on page 4: line 22 (which now follows directly after the study area description) and at the beginning of the results on page 11: line 1, where there is no longer a presentation of the data. The data discussion is now isolated to section 2.3 where we present the sensitivity experiment methods.

22. *p.8, line 18-20, see main point.*

Please see our response to the main point (1 above).

23. *p.8, line 28 to p.9, line 8, this is true. In the high river TA estuarine, $DIC:TA$ is decreased slow whereas in low river TA estuarine water, $DIC:TA$ is quickly modified and dominated by the seawater ratio. If this is the only point this paper wants to talk then why presenting the numerical model? Some of the other recent papers also talked about this point. However the assumption of same $DIC:TA$ ratio for high TA_f and low TA_f rivers are likely problematic. Not sure how meaningful is this scenario simulation.*

We are confident that a revision will clearly focus on our key points listed above and that our new scenarios and presentation will facilitate this focus. Also, our addition of model results (which are subject to the dynamics - sources/sinks within the estuary) to the figures presenting the theoretical mixing curves (see Editor response - X) will clearly show the utility of the numerical model.

We have overlaid model results on top of these theoretical curves and emphasized that the curves are only there to help interpret the model, see page 12 beginning line 13. We then emphasize the importance of model biology in deviating from these curves on page 13 beginning at line 4

24. *Page 9, Line 8: "Ocean pH and Ω_A are often assumed to be coupled": Some references may be needed here to support this. I think the word "coupled" and "decoupled"*

are misused here. In some sense, pH and omega are always coupled. They are just not “coupled” in a simple way as our “intuitions” may suggest. The simple case here is that $[Ca^{2+}]$ increased as salinity increases, but that has no direct effect on pH. There are other more subtle factors or processes influencing pH and omega differently. However I do not think we can simply call that as “decoupled”. You can find a better name.

Noted. In the new manuscript we will not use the word “coupled” but instead note that non-experts often assume lower pH implies lower Ω_A .

We no longer use the word “coupled” and now use either “asynchronous” or “trend reversal” See page 12 beginning at line 30.

25. *p.9, line 12-14 is not clear.*

Noted. In the new manuscript we will expand and clarify as this is a key point of the paper.

26. *p. 10, I like the discussion on seasonality, but it is based on physics (TA_f and discharge only).*

We will remove this section as we will focus on the Fraser River.

27. *p.10, line 14-16, true that high river TA_f systems like the Mississippi provide a strong buffer effect and its delta-pH shouldn't change as much as that in low TA_f systems during mixing. However biological production could raise pH to a very high value in the Mississippi.*

Good point. The new manuscript will focus on the Fraser River.

We have removed our discussion of other estuaries

28. *Fig. 6c and d, Note there are two arms of DIC:TA ratio to TA with a minimum at seawater TA. There is nothing magic here but the authors should mention the reason. The left reflects the mixing between the generally high ratio in river with a low ratio in seawater. The right arm reflects the mixing of a few very high TA rivers (with TA higher than the seawater) with seawater.*

As we will focus the new manuscript on the Fraser River, we will remove Figure 6d.

We have removed panel d

29. *p.11, line 1 and 6 are not consistent. Warming allow more CO_2 degassing and decreases river DIC. Yes, I agree. But increased atmospheric CO_2 probably won't increase DIC as river DIC is so much higher than the atm- pCO_2 . If there is any increase it likely increases TA equally (through increase of weathering rate).*

In the new manuscript we will only consider the Fraser River and future climate changes we are sure about, for example, changes in timing of the freshet.

We have reworded the discussion more broadly to consider general increases in the dissolved CO_2 of either endmember, see page 17: line 30

30. *p.10-11, I think this section is very speculative and should be deleted or combined into earlier discussion with short sentences. These speculations do not help, e.g.,*

we do not know which competing factor will dominate and if river DIC will increase. Overall as the authors agree that these effects are rather small comparing with eutrophication induced surface biological production and subsurface respiration induced pH changes.

In the new manuscript we will only consider future climate changes we are sure about, for example, changes in timing of the freshet.

We now only consider changing physical flow regimes and increasing dissolved carbon. We can tie both of these processes directly to our key points, and they are clearly illustrated in our new summary figure, Fig. 6. Fig. 6 also shows the magnitude of sensitivity is not insignificant relative to processes like eutrophication.

31. *p.11-12, I generally do not like long summary, which essentially does more repeating discussion.*

The summary will be focused on the key points list above and we will ensure it is not repetitive.

We have completely rewritten the conclusions to more concisely address our key points

32. *Finally, regarding pH scale. I do not understand why the authors switches between NBS and total scales. I'll stick with one and note there is big uncertainty in either one when salinity is extreme (that is pH_T doesn't work for river water and pH_{NBS} doesn't work fully for seawater). Also, pH was given as in "NIST units". This is not the right way we marine chemists will say. It should be in "NIST scale" (I would just call it "in NBS scale"). When saying a pH change then you can say "a change of 0.xx pH units". There is not such a name called NIST or NBS or total units. It is scale!*

We will use only the total scale for pH and convert all freshwater pH to total scale before presenting them in the manuscript. We will not call them units.

Use use the total scale exclusively in our revision.

33. *Since the ms is an open access discussion paper, I also asked a colleague who knows statistics better than me to read it. Below is her comments. I have read these and generally agreed.*

Page 6 Line 10: the positive bias, root-mean squared error of the model output is 0.16 for pH and 0.51 for the saturation state of aragonite. The authors claim that these errors are sufficiently small to support the model use for the process studied in the paper. I am not sure about this claim. The error of 0.51 looks big enough to me from my understanding of acidification impacts. The model may be good in reproducing the physical field and biology bloom as the authors stated here.

A regression with R^2 of 0.1 without a P value is impossible for readers to judge whether the regression is significant or not (Fig. 3b). If the regression is not significant, TA is not flow dependent, and then the model can't use this relation to derive a scenario. For the regression-based scenarios, since data vary greatly, uncertainties associated with these regressions should be provided and transferred to the model outputs. Without knowing the uncertainties, considering the error of the

model output of the saturation state of aragonite, 0.51, not so small, it is hard to evaluate the duration of $\Omega_A < 1$ in any scenario. The authors may specify how low Ω_A is in these scenarios.

Figure 3b and all TA data collected using outdated methods or in freshwater where organic alkalinity uncertainty is high will be removed. We will define new sensitivity scenarios to include more recent and newly acquired data where possible and reduce (and sometimes remove) the dependence on data in which we have less confidence (such as data collected using outdated methods or river TA with high organic alkalinity uncertainty). We will also base our flow-dependent scenarios based on theoretical weathering curves spanning the range of observations rather than statistical fits. We will re-run all the simulations with these new scenarios.

The model Ω_A uncertainty of 0.51 is large as reviewer 2 mentions, but also positively biased and thus does not overestimate the severity of aragonite undersaturation. We will reword our discussion of the model evaluation to emphasize the bias rather than the uncertainty as our motivation to go forward using the model in this study.

- **We have revised the model evaluation section to give more detail. See our response to 16 above.**
- **We have only proposed a single flow dependent scenario for our revised sensitivity analysis. We do not have enough data to demonstrate statistical significance, but, provided our assumption that TA is approximately conservative across the lower salinity range where we don't have data, then we have high confidence in our higher salinity data since we're involved in its collection, and that confidence translates to the errorbars shown in Fig. 2.**

The sensitivity of estuarine aragonite saturation state and pH to the carbonate chemistry of a freshet-dominated river

Benjamin L. Moore-Maley¹, Debby Ianson^{1,2}, and Susan E. Allen¹

¹Department of Earth, Ocean and Atmospheric Sciences, University of British Columbia, Vancouver, British Columbia, Canada

²Fisheries and Oceans Canada, Institute of Ocean Sciences, Sidney, British Columbia, Canada

Correspondence to: Benjamin Moore-Maley (bmoorema@eoas.ubc.ca)

[Add](#) [Remove](#) [Remove citation](#)

Abstract.

Ocean acidification threatens to reduce pH and aragonite saturation state (Ω_A) in estuaries, potentially damaging their ecosystems. However, the impact of highly variable river total alkalinity (TA) and dissolved inorganic carbon (DIC) on pH and Ω_A in these estuaries is unknown. We assess the sensitivity of estuarine surface pH and Ω_A to river TA and DIC chemistry using a ~~1-dimensional, biogeochemical-coupled~~ coupled biogeochemical model of the Strait of Georgia on the Canadian Pacific coast and ~~generalize~~ place the results in the context of global rivers. The productive Strait of Georgia estuary has a large, seasonally variable freshwater input from the glacially fed, undammed Fraser River. Analyzing TA and pH observations from this river plume and pH from the river mouth, and its estuary we find that the Fraser is moderately alkaline (TA 500–~~1350~~1000 $\mu\text{mol kg}^{-1}$) but relatively DIC-rich, ~~especially during winter (low flow)~~. Model results show that estuarine pH and Ω_A ~~while~~ are sensitive to freshwater DIC and TA, but do not vary in synchrony except at high DIC:TA. The asynchrony occurs because increased freshwater TA is associated with increased DIC, which contributes to an increased estuarine DIC:TA, reducing pH, while the carbonate portion of the (higher) DIC causes an increase in estuarine Ω_A . ~~Instead, rivers with high DIC and TA produce lower estuarine pH due to an increased estuarine DIC:TA ratio, but higher estuarine Ω_A because of DIC contributions to the carbonate ion.~~ When freshwater DIC:TA increases (beyond ~ 1.1), the shifting chemistry causes a paucity of the carbonate ion that overwhelms the simple dilution/enhancement effect. At this high DIC:TA ratio, estuarine sensitivity to river chemistry increases overall. Furthermore, this increased sensitivity extends to reduced flow regimes, that are expected in future. Significantly modulating these negative impacts is the seasonal productivity in the estuary which draws down DIC and reduces the sensitivity of estuarine pH to increasing DIC during the summer season. ~~This estuarine pH sensitivity decreases with increasing mean river TA, but the zone of maximum pH sensitivity also moves to higher salinity which could impact a larger areal extent of the estuary. Many temperate rivers, such as the Fraser, are expected to experience weaker freshets and stronger winter flows under climate change, reducing the extent of the river plume and the impact of river chemistry in much of the estuary. However, increasing carbon in rivers will move the highest sensitivity zone to higher salinities that cover larger areas under present-day flow regimes.~~

1 Introduction

Estuaries support productive ecosystems (Cloern et al., 2014) and significant human populations (Cloern et al., 2015). Critical trophic links within many of these ecosystems may be negatively impacted by increases in dissolved inorganic carbon (DIC) and reduced pH associated with ocean acidification (Haigh et al., 2015). Those organisms using the calcium-carbonate mineral form aragonite in their external hard parts (e.g., mussels, oysters, geoduck) are especially vulnerable since oceanic CO₂ uptake lowers the aragonite saturation state (Ω_A) of seawater (Waldbusser et al., 2015). While carbonate system dynamics and/or acid-base chemistry have been studied extensively in marine (e.g., Jiang et al., 2015) and freshwater (e.g., Schindler, 1988) environments, less is known about carbon chemistry in the diverse estuaries where these two zones meet (Salisbury et al., 2008; Hagens and Middelburg, 2016; Cai et al., 2017).

Estuarine systems are complex, cover large salinity ranges that challenge current measurement techniques and are generally under-sampled (Ianson et al., 2016; Cai et al., 2017). The carbonate chemistry in the rivers that feed these estuaries may also be exceptionally variable (Cai et al., 1998), ranging from rivers with low DIC to total alkalinity (DIC:TA) ratios and high pH (> 8) like the Mississippi River (Hu and Cai, 2013) to blackwater rivers that have low pH (< 5) (Cai et al., 1998; de Fátima F. L. Rasera et al., 2013). Along a salinity gradient there may exist maximum sensitivity zones ~~occurring where DIC~TA~~ (Egleston et al., 2010) that are especially vulnerable to acidification. The strength and location of these zones depend on the river endmember carbonate chemistry (Hofmann et al., 2009; Hu and Cai, 2013; Xue et al., 2017). This sensitivity is generally expected to increase as the ocean absorbs CO₂ and becomes warmer (Hagens and Middelburg, 2016).

In addition, seasonality is often strong and single rivers and estuaries may experience highly variable conditions in space and time (Hellings et al., 2001; de Fátima F. L. Rasera et al., 2013; Waldbusser and Salisbury, 2014; Hunt et al., 2014; Voss et al., 2014; Ianson et al., 2016; Xue et al., 2017). Carbonate and silicate weathering are major sources of river DIC and TA in most rivers (Meybeck, 1987; Amiotte Suchet et al., 2003). ~~Both quantities can be strongly flow-dependent due to dilution if physical weathering outpaces chemical weathering rates (i.e., kinetic-limited weathering (West et al., 2005)).~~ Carbonates are concentrated globally in the northern mid-latitudes (Amiotte Suchet et al., 2003), and several carbonate-rich, mid-latitude watersheds demonstrate high TA and large TA flow-dependence such as the Changjiang and Mississippi Rivers (Cai et al., 1998). TA flow-dependence is also common among low-TA, low-latitude rivers like the Amazon (Richey et al., 1990) and Congo (Wang et al., 2013) Rivers, although organic carbon contributions can complicate this behavior. In the Congo River for example, TA is flow-dependent but DIC is persistently high year-round (Wang et al., 2013). On top of natural variability, many estuaries also experience heavy anthropogenic pressure (Frankignoulle et al., 1996; Zhai et al., 2007; Cai et al., 2017), making them particularly vulnerable to ocean acidification (Cai et al., 2011, 2017) and in some cases the subject of intensive management and policy initiatives (Fennel et al., 2013).

~~DIC and TA vary by nearly two orders of magnitude between major world rivers (Cai et al., 1998), and throughout individual watersheds in space and time. Pollution can also contribute enormously to TA and DIC throughout urbanized watersheds (e.g., Scheldt and estuaries (e.g., Changjiang~~

In the present study, we determine the sensitivity of Ω_A and pH in a large, mid-latitude, fjord estuary (Strait of Georgia, Canada) to changes in freshwater TA and pH DIC using a quasi one-dimensional biogeochemical model. This model mechanistically parameterizes horizontal two-dimensional estuarine flow as a function of river flow. Few carbonate data exist in the river plume region and fewer still at the river mouth, motivating us to perform these broad analyses. We establish a freshwater TA and pH range and flow dependent variability for the system by extrapolating TA observations from the Fraser River plume region (de Mora, 1983; Ianson et al., 2016) to zero salinity. and by using We use autonomous pH measurements from an Environment and Climate Change Canada (ECCC) mooring near the Fraser River mouth We use TA and pH with our estimated TA to constrain freshwater DIC, since we lack reliable direct DIC observations in the Fraser River. From the model estuarine Ω_A and pH results across 18 river chemistry scenarios and 12 recent hydrological annual cycles based on these estimated freshwater TA and pH ranges, we identify regions of the freshwater carbonate chemistry range, expressed as both pH(DIC:TA range and DIC-TA, that produce enhanced estuarine pH and Ω_A sensitivity to this freshwater chemistry-TA. We characterize these regions in terms of (past) higher pH low DIC and (future) (lower pH) high DIC freshwater carbonate chemistry and show how conditions in this temperate estuary deviate from theoretical mixing curves due to the strong local seasonal biological cycles. We further discuss the implications of these results for global rivers and future climate with emphasis on the anticipated changes in hydrological cycles.

2 Methods

2.1 Study area

The Strait of Georgia (Fig. 1) is a large ($\sim 6800 \text{ km}^2$, $>400 \text{ m}$ deep), temperate, semi-enclosed, fjord-like estuarine sea with strong seasonal stratification, productivity, and carbonate chemistry cycles (Moore-Maley et al., 2016; Ianson et al., 2016). This high productivity supports abundant populations of shellfish, finfish, and other higher organisms that may be sensitive to pH and Ω_A anomalies (Haigh et al., 2015). The Fraser River, the primary freshwater source, drains approximately $238,000 \text{ km}^2$ with seasonally variable discharge (~ 800 to $12,000 \text{ m}^3 \text{ s}^{-1}$ at Hope, ECCC data, <http://wateroffice.ec.gc.ca>) due to summer snow/ice melt and lack of dams throughout most of the watershed. This large freshwater flux is partially contained by narrow passages and tidal mixing over sills (Pawlowicz et al., 2007), and thus imparts a significant freshwater influence on the Strait especially compared with regions where large rivers meet the ocean directly such as the nearby Columbia River plume region (Roegner et al., 2011). These same coastal and topographic features create long residence times, causing carbon to accumulate and making the Strait DIC-rich relative to the open ocean (Ianson et al., 2016) despite a strong, seasonal DIC upwelling signal over the outer shelf (Bianucci et al., 2011). The large freshwater footprint, together with the abundance of previous circulation (e.g., LeBlond, 1983; Pawlowicz et al., 2007), ecology (e.g., Masson and Peña, 2009; Allen and Wolfe, 2013), and acidification studies (e.g., Moore-Maley et al., 2016; Ianson et al., 2016) make the Strait an ideal system for investigating the response of estuarine pH and Ω_A to freshwater carbonate chemistry in a complicated estuarine setting.

The seasonal progression of productivity in the Strait of Georgia begins with a characteristic spring phytoplankton bloom (Allen and Wolfe, 2013) followed by a shallow ($\sim 20 \text{ m}$) surface layer of productivity throughout the summer that transitions

into weaker fall blooms before returning to the background winter state (Harrison et al., 1983). Below this productive surface layer, the DIC-rich intermediate basin is persistently aragonite undersaturated. This signal is mixed to the surface throughout winter, but summer productivity maintains high pH and aragonite supersaturation in the top 20 m of the water column (Ianson et al., 2016). The strength and timing of this seasonal DIC cycle is strongly linked to local wind, irradiance, and freshwater forcing, the latter of which maintains the strongest influence of the three during summer (Moore-Maley et al., 2016).

The Fraser River watershed spans four distinct geologic belts (Fig. 1a) that transition from the carbonate-rich Foreland Belt to the silicate-rich Coast Belt (Cameron and Hattori, 1997). Carbonate and silicate weathering thus dominate the watershed (Voss et al., 2014); carbonate weathering generally produces TA faster than silicate weathering (Meybeck, 1987). Observed Fraser River TA (~~Jul/Aug-2009, Oct-2010, May/June-2011, (Voss et al., 2014)~~) varies strongly throughout the watershed, but generally accumulates along the Foreland Belt, decreases along the Coast Belt, and is highest at low flow stage (Voss et al., 2014). Fraser River TA thus appears to be produced primarily by carbonate weathering in the upper watershed, diluted by weakly-buffered low-TA seaward tributaries, and flow dependent. There are no data in the Fraser River region to date that determine if organic acids and bases that may contribute significantly to TA, as they do in some coastal areas (Cai et al., 1998; Koeve and Oschlies, 2012; Kim and Lee, 2009; Hernández-Ayón et al., 2007) and rivers (Hunt et al., 2011; Kennedy, 1965). carbonate alkalinity estimates (which are required to calculate DIC) become increasingly inaccurate. Carbonate alkalinity is estimated to be as low as 10% of TA in the Congo (Wang et al., 2013) and Kennebec Rivers (Hunt et al., 2014). ~~The carbonate alkalinity fractions of TA in the Fraser River and Strait of Georgia are unknown.~~

~~Data sources~~

~~(This section has migrated to Sec. 2.3. Discussion of organic alkalinity has migrated to Sec. 2.1.)~~

2.2 Model

2.2.1 Overview

In order to resolve the primary productivity in the strongly stratified Strait of Georgia, it is necessary to have fine vertical resolution but it is not necessary to model the whole water column. Given the summer depth of the chlorophyll maximum of 5 m (Peña et al., 2016) and typical mixing layer depths of 1-7 m (Collins et al., 2009), we use 0.5 m vertical resolution and model the upper 40 m. The vertical model is located directly to the northwest of the Fraser River plume region (Fig 1b). The region of the Fraser plume is dominated by estuarine circulation and wind-mixing. The dynamics have been well-studied (e.g., Pawlowicz et al., 2007) giving us the information to effectively parameterize higher dimensional processes with a one dimensional (1-D) model (Collins et al., 2009; Allen and Wolfe, 2013). The benefits of a 1-D model are the quick run times that allow us to simulate many parameter variations over multiple annual cycles (Moore-Maley et al., 2016).

Accurately simulating mixing of the stratified plume with the waters below is required to reproduce the biology and chemistry of the plume. To this end, the physical model is based on the KPP mixing-layer model which includes the impacts of winds and heat/cooling on currents and mixing (Large et al., 1994). We add baroclinic pressure gradients and estuarine circulation

to the model. More specifically, we add (1) freshwater and freshwater tracers to the mixing layer of the model, (2) a vertical upwelling due to entrainment and (3) a seaward advective loss to conserve volume flux. All three are defined in terms of the total freshwater discharge from the Fraser River and other small rivers (Collins et al., 2009).

The model represents a column of water with radius about one tidal excursion. It uses a 15 minute timestep. ~~We employ a one-dimensional (1-D), biogeochemical-coupled, Strait of Georgia mixing model that resolves the upper 40 m of the water column and predicts annual cycles (Moore-Maley et al., 2016) in order to investigate the sensitivity of surface estuarine pH and Ω_A in the Strait to changes in river carbonate chemistry. Three-dimensional estuarine circulation is parametrized as an upward entrainment velocity and outward advective flux, both. The advective loss arises due to water column convergence, since the upward entrainment velocity increases with depth.~~ We explicitly model *in situ* temperature, ITS-90 (Preston-Thomas, 1990), and practical salinity, PSS-78 (UNESCO, 1981), as physical state variables.

The biological model contains three nutrient classes (nitrate, ammonium, dissolved silica), three photosynthesizer classes (diatoms, ~~heteromixotrophs~~ as *Mesodinium rubrum*, nanoflagellates), three grazer classes (*M. rubrum*, microzooplankton, mesozooplankton), and three detritus classes (dissolved and particulate organic nitrogen, biogenic silica). *M. rubrum* (a ciliated protozoan) retains functional chloroplasts during grazing and uses them to perform photosynthesis. Calcifying phytoplankton (e.g., coccolithophores) are assumed to contribute minimally to productivity in the Strait of Georgia (Haigh et al., 2015) and were absent from satellite observations in the Strait prior to 2016 (J. Gower, personal communication, 2014; NASA Earth Observatory, <http://earthobservatory.nasa.gov/IOTD/view.php?id=88687>) – they are not explicitly modeled.

DIC and TA are both explicitly modeled and are coupled to the biological growth and remineralization cycles (Moore-Maley et al., 2016). Transfer of CO_2 across the air-sea interface in the surface grid cell is parametrized according to Fick's second law of diffusion (Sarmiento and Gruber, 2006), using gas transfer coefficient (Nightingale et al., 2000), Schmidt number (Wanninkhof, 1992), and K_0 solubility coefficient (Weiss, 1974) parameterizations. Model pH (total scale) and Ω_A are calculated from model DIC, TA, dissolved silica, temperature, salinity, pressure, and estimated phosphate using the CO2SYS program (Lewis and Wallace, 1998) and full salinity range K_1 and K_2 constants (Millero, 2010). Phosphate is roughly approximated ($\pm 1 \mu\text{mol kg}^{-1}$, Riche (2011)) from model nitrate using the Redfield N:P ratio. Calcium ion concentrations, required for Ω_A calculation, are approximated by a linear regression to salinity (Riley and Tongudai, 1967), and by the mean observed calcium ion concentration near the Fraser River mouth, $350 \mu\text{mol kg}^{-1}$ (Voss et al., 2014), where salinity < 1 .

2.2.2 Initialization and forcing

We use profiles of temperature, salinity, fluorescence, chlorophyll *a*, nitrate, and dissolved silica (1999 through 2012) measured near the model site (Pawlowicz et al., 2007; Masson, 2006; Masson and Peña, 2009; Peña et al., 2016) (D. Masson, personal communication, 2014) to initialize the model (see Moore-Maley et al., 2016). Model runs are initialized in autumn and run through a full year and then beyond until the end of the following December. Our analysis starts at the beginning of the year following the initialization date which is always a longer period than the 30-day spin-up period. Initial phytoplankton, zooplankton, and detritus concentrations are determined according to Moore-Maley et al. (2016). Since few DIC and TA data are available, we use a representative fall profile (11 September, 2011 (Ianson et al., 2016)) to initialize model DIC and

TA. Model pH and Ω_A are not sensitive to initial carbonate chemistry conditions after the spin-up period. Time-averages (fluorescence, chlorophyll *a*, nitrate, dissolved silica) and annual fits (temperature, salinity, DIC, TA) of the initialization data near 40 m are used to set the 40 m boundary conditions (Moore-Maley et al., 2016). Average model 40 m boundary conditions are summarized as the model seawater endmember in Table 1.

5 The model is forced at the surface (Allen and Wolfe, 2013) by wind stress calculated from hourly wind speed and direction observed at Sandheads weatherstation, and by heat fluxes derived from cloud fraction, air temperature and relative humidity observed at Vancouver International Airport (Fig. 1b; ECCO observations, <http://climate.weather.gc.ca/>). Total freshwater flux (volume/time) into the Strait of Georgia is prescribed (Allen and Wolfe, 2013) using daily river discharge measurements obtained by ECCO (<http://www.wateroffice.ec.gc.ca/>) in the Fraser River at Hope and in the Englishman River at Parksville
10 (Fig. 1b). Englishman River discharge is used in this study as a proxy for the contribution of small, rainfall-dominated rivers to the freshwater budget of the Strait (Collins et al., 2009). Heat and nutrient fluxes due to freshwater are prescribed (Moore-Maley et al., 2016) as concentration \times flux. Model freshwater endmember concentrations are summarized in Table 1 Concentration values used similarly for TA and DIC are discussed in Sect. 2.3.

2.2.3 Evaluation

15 Previous studies using the model have evaluated it against physical, biological and chemical data. The vertical profiles of density and in particular, the depth of the halocline are well represented (Collins et al., 2009). The model captures interannual variability in the biology and in the physics driving the biological variability – the model accurately predicts the timing of the spring phytoplankton bloom (Allen and Wolfe, 2013; Allen et al., 2016). The large seasonal variation of the carbon cycle is captured with some underestimation of DIC in the summer due to over-productivity (Moore-Maley et al., 2016) a common
20 problem with coupled models in the Strait of Georgia (e.g., Peña et al., 2016). The resulting positive-bias, root-mean-squared error (RMSE) is 0.16 for pH and 0.51 for Ω_A (Moore-Maley et al., 2016), sufficiently small to support its use for the process studies described here. Evaluation of pH and Ω_A in the model shows both systematic and non-systematic errors (Moore-Maley et al., 2016). The variations in pH observations are well captured by the model with a correlation coefficient of 0.80. There is a positive bias which is higher at high pH. The root-mean-squared error (RMSE) for pH is 0.16 but removing the systematic
25 error (by fitting a line between the model and observations) gives a non-systematic or scatter RMSE of 0.06. One-third of this discrepancy can be explained by mismatches between model time and space. The evaluation is similar for Ω_A , correlation of 0.79, a RMSE of 0.51 with a scatter RMSE of 0.18, and average mismatches due to time and space of 0.05. Thus, the non-systematic error is sufficiently small to support the model's use for the process studies described here. Note that the systematic bias means that the model is conservative, over-predicting both pH and Ω_A .

30 2.3 Sensitivity analysis

TA can behave, at times, like a conservative tracer in the Canadian coastal Pacific Ocean (Ianson et al., 2003). We therefore estimate the Fraser-dominated, seasonal, freshwater TA endmembers for the Strait of Georgia by extrapolating TA observations from 10 sampling cruises. In order to test the sensitivity of the biogeochemical model to changes in freshwater chemistry, we

select ranges of freshwater TA and DIC endmembers based on observed TA in the Fraser plume and pH near the Fraser River mouth. We extrapolate estuarine TA data (Ianson et al. (2016), Table S1) sampled throughout the water column, following modern sampling and analysis procedures (Dickson et al., 2007), from seven recent (2010–2016) sampling campaigns near the Fraser River plume (Fig. 1b) (de Mora, 1983, Ianson et al., 2016) and Table ??) to zero salinity ($S=0$) using linear regression
5 in order to establish freshwater TA endmembers across multiple seasons (Fig. 2a). We only consider profiles ~~or transects~~ that include at least one TA sample below ~~$S=20$ to ensure~~ a salinity of 20 to allow sufficient river influence, ~~which limits our analysis to 5 cruises prior to 1980 (March, May, October 1978 and January, April 1979; (de Mora, 1983)) and 5 cruises after 2010 (August, October 2010, June, August 2011 and July 2012; (Ianson et al., 2016)).~~

Unlike TA, DIC does not behave conservatively in the Strait of Georgia. We therefore calculate the freshwater DIC endmember
10 from the extrapolated TA endmembers and a Fraser River pH range determined using DIC can vary at constant pH, however DIC:TA cannot (given constant temperature and salinity). Thus rather than prescribing freshwater DIC directly, we define freshwater DIC:TA endmembers based on observations from the ECCC Fraser River Water Quality Buoy (Fig. S1) moored approximately 10 km upstream ~~along the main arm~~ of the river mouth (Fig. 1b). Buoy pH was measured potentiometrically using a regularly-inspected (bimonthly to monthly), hull-mounted, YSI ADV6600 multisensor and recorded hourly ~~on the National~~
15 ~~Institute of Standards and Technology (NIST) scale between 2008 and 2013~~ from 2008 until present (Ethier and Bedard, 2007). We calculate DIC ~~from TA and~~ from buoy pH using the CO2SYS program (Lewis and Wallace, 1998) and full salinity range K_1 and K_2 constants (Millero, 2010).

There are uncertainties associated with the extrapolated freshwater TA endmembers due to our assumptions that TA is conservative across such a wide salinity range and that organic alkalinity contributions in the Fraser Plume region are small. There
20 are also significant uncertainties in the freshwater pH observations given that potentiometric pH measurements in ~~sea~~ freshwater are generally no more precise than 0.02 units (Byrne et al., 1988; Dickson, 1993), ~~however inconsistencies in electrode type and calibration can produce errors in freshwater larger than~~ 0.2 units (Covington et al., 1983). A thorough error analysis of these data is intractable given the paucity of data and our lack of additional parameters such as $p\text{CO}_2$. Instead, given these uncertainties, we consider the extrapolated freshwater TA endmembers, ~~the buoy pH record,~~ and the ~~resulting calculated~~ freshwater
25 DIC:TA endmembers calculated from the buoy pH record to represent approximate seasonal ranges of freshwater carbonate chemistry rather than absolute values. ~~To provide context to these TA ranges, we compare our endmembers to TA data from ECCC Fraser River sampling programs near the ECCC Water Quality Buoy and approximately 100 km upstream near the town of Hope, BC (Fig. 1; Table ??). Since neither dataset was sampled to oceanographic standards — specifically samples were unpreserved and stored in polyethylene containers — we use these data for comparison only and not to define our freshwater~~
30 ~~carbonate chemistry endmembers.~~

In order to determine the sensitivity of estuarine pH and Ω_A to freshwater TA and pH, we define approximate minimum, mean, and maximum freshwater TA (TA_f) and pH (pH_f) scenarios based on the freshwater endmembers that we estimate from the data discussed in Sect. ?. As seasonal variations in freshwater TA are likely flow-dependent, we define an additional three flow-dependent TA_f scenarios using TA-discharge regressions of the extrapolated endmembers and the two ECCC comparison
35 datasets discussed in Sect. ?. We calculate freshwater DIC (DIC_f) from TA_f and pH_f according to Sect. ?.

The freshwater TA endmembers span an approximate range between 500 and 1000 $\mu\text{mol kg}^{-1}$ (Fig. 2). We thus define five constant freshwater TA (hereinafter TA_f) scenarios: three at the minimum, center and maximum of the extrapolated endmember range (500, 750 and 1000 $\mu\text{mol kg}^{-1}$, respectively) and two more to represent extremes beyond our estimated range at 250 and 1250 $\mu\text{mol kg}^{-1}$ (Table 2). The extrapolated endmembers also vary seasonally, demonstrating significant hysteresis with respect to Fraser River discharge at Hope (lowpass filtered with a 40-day cutoff, Q_{filt} , Fig. 2b) and a positive correlation to dQ_{filt}/dt (Fig. 2c). We thus add an additional flow dependent TA_f scenario based on a linear regression of the extrapolated TA endmembers to dQ_{filt}/dt given by

$$\text{TA}_f = \frac{\text{TA}_0 t_0}{Q_0} \frac{dQ_{filt}}{dt} + \text{TA}_0 \quad (1)$$

where $\text{TA}_0 = 750 \mu\text{mol kg}^{-1}$, $Q_0 = 840 \text{ m}^3 \text{ s}^{-1}$ and $t_0 = 86400 \text{ s}$ (Table 2).

Buoy pH is seasonally variable (Fig. S1) and changes are likely driven primarily by biological productivity since the correlation to river discharge is weak and summer river warming would tend to drive pH seasonal cycles in the opposite direction. The complete buoy pH record follows a Gaussian distribution with a median of approximately 7.5 and first and 99th percentiles at approximately 7.1 and 7.9, respectively (Fig. S1). Over the annual model freshwater temperature range (2.5-19.3°C) these pH values, in order from highest to lowest, correspond to average DIC:TA values of 1.032, 1.089, and 1.226. We use these freshwater DIC:TA values (hereinafter $\text{DIC}_f:\text{TA}_f$) as our respective Low Carbon, Med Carbon, and High Carbon freshwater endmember cases (Table 2). The Low Carbon case ~~We use a high-pH_f scenario of 8.0 total scale units, which is the upper end of the observed buoy pH and~~ is typical of present-day high TA rivers with low DIC:TA such as the Mississippi (Cai, 2003) and Changjiang (Zhai et al., 2007) Rivers. We suggest that this scenario represents ~~an upper~~ lower limit in the Fraser River and may represent past chemistry (lower $p\text{CO}_2$). Likewise, we ~~define a low-pH_f scenario of 7.4 units~~ consider the High Carbon case to represent possible future $p\text{CO}_2$ increases but still within the range of present-day Fraser River pH observations (buoy pH). This ~~low-pH_f~~ High Carbon scenario still has a lower $\text{DIC}_f:\text{TA}_f$ than low pH, weakly-buffered rivers such as the Kennebec (Hunt et al., 2014) and Congo (Wang et al., 2013) Rivers. These three $\text{DIC}_f:\text{TA}_f$ cases combined with our six TA_f cases produce 18 individual river endmember chemistry scenarios that we use in the biogeochemical model (summarized in Table 2).

For each permutation of TA_f and $\text{DIC}_f:\text{TA}_f$ ~~and pH_f scenario~~, we ran the model ~~for 12 separate years: 2001 to 2012~~ over the same 12-year period (2001–2012) used in previous studies involving this model (e.g., Moore-Maley et al., 2016) to maintain consistency with previous work and to ensure a wide range of climatological forcing regimes. With 18 possible ~~TA_f and pH_f~~ combinations of TA_f and $\text{DIC}_f:\text{TA}_f$, we ran the model a total of 216 times. Since the seasonality of ~~pH and~~ DIC and TA in the Strait of Georgia is surface-intensified (Moore-Maley et al., 2016), we use surface (3 m average) DIC:TA ratio, pH and Ω_A ~~aragonite undersaturation ($\Omega_A < 1$) duration~~ as our primary model sensitivity metrics. ~~At constant salinity and temperature, pH and DIC:TA vary inversely. We average surface DIC:TA and pH over two different salinity regimes: $S < 20$ (summer) and $S \geq 20$ (remainder of the year). Since the model demonstrates periods of $\Omega_A < 1$ in winter and strong freshet summers (Moore-Maley et al., 2016), we evaluate $\Omega_A < 1$ duration during both seasons.~~

3 Results

Data analysis and sensitivity scenarios

The freshwater TA endmembers extrapolated from the Fraser plume cruise data (Table ??; Fig. ??) span a range of approximately 500 to 1350 $\mu\text{mol kg}^{-1}$ and demonstrate a significant negative correlation to discharge, although freshwater TA increases slightly above 7,000 $\text{m}^3 \text{s}^{-1}$ (open symbols, Fig. ??a). Observed TA from the cruise data at zero salinity ($S = 0$) are generally slightly higher than the endmembers because of the non-conservative behavior of TA in the Fraser River at low salinity (filled symbols, Fig. ??a). The ECCC comparison TA data from the Fraser rivermouth and ~ 150 km upstream at Hope described in Sect. ?? (Table ??) cover similar ranges and also negatively correlate with discharge (Fig. ??b and c).

Buoy pH varies seasonally from approximately 7.4 to 8.0 NIST units between low flow and peak flow (disregarding sporadic readings below 7.4 and above 8.0), and is positively correlated to river discharge except at higher flow where it reaches a maximum (Fig. ??d). However, since the correlation is weak and the cycles of river discharge and primary productivity (low in winter, high in summer) are in-phase, the pH variability in the lower Fraser River is likely driven primarily by local processes that influence DIC such as phytoplankton growth rather than changes in river flow. The buoy pH cycle is consistent with such a biologically-driven cycle, whereas, the seasonal temperature cycle would drive pH changes in the opposite direction. The typical winter to summer temperature increase (maximum ~ 2 to 20°C) would cause a decrease in pH of ~ 0.15 pH units in summer.

We define our three constant TA_f scenarios to span the range shown by our freshwater TA endmembers: minimum $\text{TA}_f = 500 \mu\text{mol kg}^{-1}$, mean $\text{TA}_f = 900 \mu\text{mol kg}^{-1}$, and maximum $\text{TA}_f = 1350 \mu\text{mol kg}^{-1}$ (Table 2). We further define our three flow-dependent TA_f scenarios based on the TA-discharge, least squares regressions of the freshwater TA endmembers (Endmember Fit) and the ECCC comparison datasets (Rivermouth Fit and Hope Fit; Fig. ??a-c) for a total of six TA_f scenarios (Table 2). Our TA_f scenarios cover the total observed range over multiple years, and we assume that, despite uncertainty in some of the data (Sect. ??), they include realistic variability.

We define our three constant pH_f scenarios (Table 2) to span the range shown by the buoy pH record, however we use the oceanography-preferred (Dickson et al., 2007) total pH scale for our estuarine analysis. The present-day scenario ($\text{pH}_f = 7.7$, total scale) is based loosely on mean NIST scale buoy pH (Fig. ??d). Given the large seasonal temperature change ($> 15^\circ\text{C}$ increase in summer), a constant pH_f implies a summer DIC_f decrease due to temperature (causing $\text{DIC}_f:\text{TA}_f$ to decrease by about 0.06) which is not as large as the observed seasonal difference because observed pH increases in summer. Our low to high pH_f scenarios (Table 2) imply $\text{DIC}_f:\text{TA}_f$ ratios of 1.10-1.13, 1.05-1.07 and 1.02-1.03, respectively, with the ranges being summer-winter values.

3.1 Sensitivity to physical forcing

Freshwater forcing exerts strong control over model biology (nutrients, light, phytoplankton, zooplankton) and carbonate chemistry (DIC, TA, pH, Ω_A), particularly during summer (Moore-Maley et al., 2016). Although the model is forced by a combination of the Fraser River and local rainfall-dominated rivers, the Fraser accounts for most of the summer signal. The Fraser

River flow record at Hope during the 12 year period from 2001 through 2012 is seasonally and interannually variable in terms of freshet size, timing, and duration with the smallest freshet (in 2010) just under $6000 \text{ m}^3 \text{ s}^{-1}$ and the largest freshet (in 2012) just under $12000 \text{ m}^3 \text{ s}^{-1}$ (Fig 3a). Model salinity (3 m averaged) is strongly inversely related to this freshwater signal and reaches a minimum of approximately 15 in 2010 and 5 in 2012 (Fig 3b). Winter rainfall pulses and their effect on winter salinity are evident particularly in February 2005. However several winter salinity dips appear without noticeable corresponding pulses in the Fraser Record. These events are likely forced by the scaled Englishman River record (not shown). Overall, aside from a handful of stronger winter salinity dips, a salinity threshold of ~ 20 appears to separate the summer high flow period from the lower background flow regime.

Model DIC:TA, pH and Ω_A (3 m averaged) during 2010 and 2012 all demonstrate strong seasonal variability between winter and summer (Fig. 4) which can be attributed to the seasonal cycle of productivity that is characteristic of the region and persistent in the model (Moore-Maley et al., 2016). Prior to the summer, differences between the two years arise primarily due to variable wind and irradiance affecting the onset and termination of spring blooms. However, the large differences between the two years in summer due to Fraser River discharge are even more apparent. Throughout the summer, biological drawdown of DIC remains strong in 2010 keeping DIC:TA low and pH and Ω_A high (red lines, Fig. 4), but DIC drawdown weakens during 2012 due to river shading caused by river turbidity, thus increasing DIC and DIC:TA and significantly lowering pH and Ω_A (black lines, Fig. 4). Meanwhile, superimposed on top of this physical-biological response, the effects of river chemistry begin to emerge. During the summer, model DIC:TA and pH vary across the 6 TA_f cases (Fig. 4a and b, gray/pink lines) by approximately half of the total difference between years (black – red) at peak freshet. This variability across TA_f cases is not evident for model Ω_A .

Considering only the flow dependent TA_f case, the strongest TA_f variations ($\sim 100\text{--}400 \mu\text{mol kg}^{-1}$) occur during the summer (Fig. 5a) due to the rapid and persistent rising and falling discharge rates associated with the Fraser River freshet (Fig 3a). Positive TA_f deviations prior to the freshet during rising water cause an overall decrease in pH and Ω_A (3 m averaged), although the timing of these events can vary depending on the freshet timing. For example, model pH and Ω_A decrease by 0.1 and 0.07, respectively, in June 2007 and May 2008 (Fig. 5b and c) due to the large TA_f increase (Fig 5a), and associated DIC_f increase, during the rapid early progression to freshet in those years (Fig 3a). In contrast, the freshet in 2012, although larger, progresses more slowly (Fig 3a) and the model pH and Ω_A decreases are thus smaller and occur at different times in the season (Fig. 5b and c). Following the freshet, negative TA_f deviations during falling water cause an overall increase in pH and Ω_A , although the increase is not as strong as the pre-freshet decrease for pH (Fig. 5b). While these changes are significant (e.g., $\Delta\text{pH} = 0.1$ and $\Omega_A = 0.07$ at times), they are small relative to the differences across the range of TA_f scenarios (Fig. 4) and practically insignificant relative to the differences between low and high flow years (e.g., 2010 and 2012, Fig. 4). Furthermore, the model pH and Ω_A deviations caused by flow-dependent TA_f are moderately symmetric about the freshet and likely time-average to the results in a constant TA_f scenario. Thus flow dependence is likely less important than other factors when considering freshwater chemistry in this system, however, it could play an important role on daily to weekly timescales.

3.2 Sensitivity analysis to river chemistry

In order to examine the response of the model across the range of TA_f for all years and across all three freshwater carbon ($DIC_f:TA_f$) scenarios, similar to our analysis of 2010 versus 2012 at Med Carbon ($DIC_f:TA_f = 1.089$, Fig. 4), it is useful to look at the model results as time averages. We identified a model salinity of 20 to be an approximate threshold separating the summer flow regime from the background flow during the rest of the year. We thus time average our results over the period
5 where salinity < 20 using the same three metrics (3 m averaged DIC:TA, pH, Ω_A) as in Fig. 4 and the same flow year color scheme as in Fig. 3 to produce a comprehensive summary of our 216 model runs across 18 freshwater chemistry scenarios and 12 years of freshwater (and wind and meteorological) forcing at low salinity (Fig. 6). The sensitivity of the model to differences in river discharge between years (e.g., red and black lines, Fig. 4) is clear in these low salinity time averages as the vertical spread of points across the color palette, with 2010 and 2012 again highlighted (red and black stars, Fig. 6). The sensitivity of
10 the model to TA_f (e.g., pink and gray lines, Fig. 4) is also clear as the trend along the horizontal axis in each panel (Fig. 6).

Time averaged (salinity < 20) model DIC appears to increase with increasing TA_f in all three river carbon cases, causing an increasing trend in model DIC:TA (Fig. 6a-c) and a decreasing trend in model pH (Fig. 6d-f). These trends are weak in the Low Carbon scenario such that the response to TA_f (difference across the range of TA_f within a given year) is weaker than the response to freshwater flow (color spread, Figs. 6a and d). Conversely, the increase in model DIC:TA and decrease in model pH
15 with TA_f in the High Carbon scenario are significantly stronger than the corresponding responses to freshwater flow (Figs. 6c and f). These results show that a high carbon freshwater endmember produces a more sensitive estuarine response than a low carbon freshwater endmember.

The response of model Ω_A to freshwater chemistry is more complicated. First of all, the dominance of freshwater flow, diluting both the calcium and carbonate ion, over freshwater chemistry in determining model Ω_A between 2010 and 2012
20 (Fig 4c) is robust throughout the 18 freshwater chemistry scenarios as evident by the large vertical color spread relative to the trends along the horizontal axis (Figs. 6g-i). Secondly, model Ω_A increases with TA_f in the Low Carbon scenario despite increasing model DIC:TA and decreasing model pH (Figs. 6a, d and g) because increasing DIC also increases the carbonate ion concentration in this case. Then in the High Carbon scenario, model Ω_A reverses its sensitivity to TA_f to follow the model pH trend (Figs. 6f and i). In this case the shift within the DIC pool to dissolved CO_2 causes a sufficient reduction in the carbonate
25 ion, overwhelming the ‘dilution effect’ described above at lower DIC:TA.

~~The sensitivity of model surface DIC:TA and pH to TA_f and pH_f is strong at low salinity ($S < 20$) which occurs during high freshwater discharge (Fig. 3), and relatively weak at high salinity ($S \geq 20$; Fig. ??e and e). As the mean annual TA_f increases in TA_f scenarios 1 through 6 (Table 2) within a given $DIC_f:TA_f$ treatment (constant pH_f ; shaded bands, Fig. ??b-g), the concurrent increase in DIC_f causes model pH to decrease by raising model DIC:TA (Fig. 6b-f). This effect is strongest at
30 $pH_f 7.4$ (Fig. 6e and d) where the range of model pH and DIC:TA across the TA_f scenarios nearly doubles relative to $pH_f 8.0$.~~

~~Model $\Omega_A < 1$ duration is 3 to 4 months in all winters, and about 1 month when it occurs in summer (nearly half of all runs; Fig. ??f and g). Both summer and winter $\Omega_A < 1$ duration are highly sensitive (> 10 day median change across all scenarios) to TA_f and pH_f . However, despite rising estuarine DIC:TA and declining pH, $\Omega_A < 1$ duration in the estuary declines with increasing TA_f . The sensitivity of this decline is strongest at $pH_f = 8.0$ (where model pH sensitivity is weakest), with the
35 largest decline between the two highest TA_f scenarios (5: Hope Fit TA_f and 6: Maximum TA_f). In the case of high pH_f~~

(8.0) in summer, the number of runs exhibiting any duration of $\Omega_A < 1$ decreased from four to one of twelve across all TA_f scenarios (Fig. ??f).

The impact of flow dependence is generally weak except at $pH_f = 8.0$ where median summer $\Omega_A < 1$ duration is reduced by ~ 10 to 15 days (Fig. ??f) between TA_f scenarios 3 and 4 (Rivermouth Fit TA_f and Mean TA_f). This reduction is consistent with higher TA_f at peak river flows in the Mean TA_f case (scenario 4) compared to the Rivermouth Fit TA_f case (scenario 3; Fig. ??b). Overall, modeled surface estuarine pH and $\Omega_A < 1$ duration are less sensitive to the range of pH_f than they are to the range of TA_f . The primary importance of pH_f , rather, appears to be as a catalyst for pH and $\Omega_A < 1$ duration sensitivity to TA_f , with the sensitivity of the two quantities strongest at opposite ends of the pH_f range.

4 Discussion

4.1 Two-endmember conservative mixing Mechanisms influencing sensitivity

To conceptualize why model estuarine 3 m average DIC:TA is highest and model pH is lowest at high TA_f (while pH_f , or $DIC_f:TA_f$ is held constant) and why this sensitivity is strongest at low pH_f , it is useful to consider the simple case of in the High Carbon scenario, we calculate conservative mixing curves between model freshwater and seawater endmembers (Table 1) at $TA_f = 500 \mu\text{mol kg}^{-1}$ (solid lines) and $TA_f = 1000 \mu\text{mol kg}^{-1}$ (dashed lines) across the Low (magenta), Med (black) and High (yellow) Carbon scenarios (Fig. 7a-c). When model daily averages in salinity space for the largest freshet year (2012) are compared to these curves, similarities in estuarine DIC:TA, pH, and Ω_A between the model and the mixing curves begin to emerge. More specifically, the variabilities of model DIC:TA, pH and Ω_A between $TA_f = 500 \mu\text{mol kg}^{-1}$ (closed circles) and $TA_f = 1000 \mu\text{mol kg}^{-1}$ (open circles) across the Low, Med and High Carbon scenarios at low (< 15) salinity (Fig. 7a-c) are in the same direction and of similar magnitude to those in the corresponding endmember mixing curves. Model pH in the High Carbon scenario (yellow circles, Fig 7b), for example, decreases by approximately 0.2 between the low TA_f and high TA_f cases similarly to the mixing curves (yellow lines). These variations with freshwater chemistry changes are analogous to the trends discussed in Sect. 3.2 (Fig. 6).

The mixing curves illustrate that increasing TA_f within a given $DIC_f:TA_f$ scenario results in a greater contribution of DIC to the estuary relative to TA. This carbon increase is seen most clearly in the difference of the DIC and TA mixing curves, DIC–TA (Fig 7d), but is also evident by comparing the DIC:TA curves between the low and high TA_f cases (Fig 7a). For DIC:TA, the endmembers are the same in both TA_f cases, but the ratio within the estuary is different. The extra DIC in the estuary is what causes pH and Ω_A to decrease with increasing TA_f , and those decreases are strongest in the High Carbon scenario (e.g., Fig. 6f and i) because $DIC_f:TA_f$ is larger so the excess DIC contribution to the estuary is higher between TA_f scenarios (yellow curves, Fig 7d).

Model Ω_A responds differently to TA_f under each of the three freshwater carbon scenarios, reversing its trend between Low Carbon and High Carbon. The mixing curves demonstrate a similar pattern (Fig. 7c) where the Med Carbon scenario appears to define a threshold at which Ω_A diverges from its similarity to pH in response to TA_f . The responses of model pH and Ω_A to freshwater carbonate chemistry changes in this system are thus asynchronous. We attribute this asynchrony to

higher estuarine carbonate in the high TA_f case which is able to buffer effectively against the equilibrium-driven carbonate loss that accompanies rising estuarine DIC:TA, but only in the Med and High Carbon scenarios. In the Low Carbon scenario, the equilibrium-driven carbonate loss is too strong.

While the trends of the model with changing freshwater scenarios are similar to those of the endmember mixing curves, the striking differences highlight the importance of biology and gas exchange in mitigating unfavorable carbonate chemistry conditions in the Fraser River – Strait of Georgia system. The model converges tightly to the seawater endmember for most of the winter, but estuarine carbon decreases dramatically during the spring phytoplankton bloom (green arrows, Fig. 7a). The model remains carbon deficient relative to the mixing curves throughout the year, only partially converging toward the freshwater endmember during the freshet. The model then retraces its carbon deficient path toward higher salinity and only converges back to the seawater endmember after fall phytoplankton blooms terminate (blue arrows, Fig. 7a). Most importantly, while biology and gas exchange do not completely buffer the effects of freshwater chemistry in the model, they do shift the system toward a significantly lower carbon state than would be found under mixing alone.

~~In the absence of biological processes and gas exchange, physical dilution alone drives linear mixing between these two endmembers, and thus the mixing curves for DIC, TA, temperature, dissolved silica, and phosphate are linear with respect to salinity (e.g., DIC and TA, Fig. ??a). However, pH calculated from these curves (CO2SYS (Lewis and Wallace, 1998)) with full salinity range K_1 and K_2 constants (Millero, 2010)) is not linear with salinity and demonstrates a characteristic minimum between the two endmembers when pH_f is lower than the seawater endmember pH (Fig. ??b). Similar theoretical salinity-pH curves have been calculated (Mook and Koene, 1975; de Mora, 1983; Whitfield and Turner, 1986; Hofmann et al., 2009; Hu and Cai, 2013) and also observed (e.g., Scheldt River estuary (Mook and Koene, 1975; Hofmann et al., 2009), Fraser estuary (de Mora, 1983)).~~

~~Estuarine pH along the mixing line is clearly sensitive to pH_f , however large differences also arise from changes in TA_f (Fig. ??b). The reason for this sensitivity to TA_f is the dramatic difference in DIC:TA along the mixing line between TA_f cases despite an equal ratio between the two cases at the freshwater and seawater endmembers (Fig. ??c). In the high TA_f case, the estuarine DIC:TA decreases more linearly with salinity resulting in a higher estuarine DIC:TA and lower estuarine pH overall. In the low TA_f case, estuarine DIC:TA decreases rapidly with salinity producing a higher estuarine pH. The difference between these curves increases with the difference between the freshwater and seawater DIC:TA endmembers (increasing $DIC_f:TA_f$, decreasing pH_f).~~

~~Despite our limited model results in the low salinity range ($S < 10$), the simple mixing case can help us explain the model sensitivity. In both the model case and the mixing case, higher TA_f (at constant $DIC_f:TA_f$) produces lower estuarine pH (Fig. ??d and e and ??b) because of the dramatic increase in estuarine DIC:TA (Fig. ??b and e and ??c). The low pH_f (high $DIC_f:TA_f$) scenarios demonstrate the strongest estuarine pH sensitivity to TA_f because they produce the largest difference between freshwater and seawater DIC:TA endmembers (Fig. ??c).~~

~~Ocean pH and Ω_A are often assumed to be coupled, however they are clearly not in brackish estuarine waters fed by rivers with moderate or low TA_f (Fig. ??d through g). This asynchrony arises because the response of estuarine carbonate ion over the large range of river TA_f and pH_f scenarios is more sensitive to changes in total DIC than shifts in the equilibrium point of~~

the carbonate system. Thus increases in model DIC (and carbonate ion) shorten $\Omega_A < 1$ duration despite reductions in estuarine pH. This carbonate mechanism is also responsible for the increased sensitivity of model Ω_A to TA_f at high pH_f . At low pH_f , the carbonate equilibrium shifts are strong enough to stabilize $\Omega_A < 1$ duration to TA_f (DIC_f) changes, but at high pH_f these equilibrium shifts are weak and DIC_f (CO_3^{2-}) increases dominate.

5 Our model sensitivity studies demonstrate the impact of freshwater carbonate chemistry on the marine environment beyond the simple bulk mixing case. Air-sea gas exchange, biological activity, dynamic mixing, and estuarine circulation make these studies more realistic, yet also more complicated. (Hofmann et al., 2009) found that adding a biogeochemical model to a prescribed physical mixing scenario in the highly polluted Scheldt estuary decreased the low-salinity pH minimum due to strong remineralization of abundant anthropogenic organic carbon (Frankignoulle et al., 1996) and increased pH at higher
10 salinity due to intense outgassing (Schiettecatte et al., 2006). In contrast the Fraser River estuary is biologically productive and deep (model site is deeper than 300 m) and much of the organic matter produced locally sinks and is remineralized well below the surface layer (Johannessen et al., 2008) resulting in increased estuarine pH across the salinity range during summer (Ianson et al., 2016) compared with the two-endmember mixing model. Still, this simplified case reproduces the overall estuarine pH sensitivity that we observe in the coupled model.

15 **Implications for other estuaries**

The sensitivity of estuarine pH to this flow dependence (seasonal TA_f variability) in the simple mixing model changes significantly with freshwater DIC and TA (ΔpH , Fig. ??d). This sensitivity is large ($\Delta pH > 0.1$) and centered at low salinity (8-10) over the Fraser River TA_f range (500-1,350 $\mu eq kg^{-1}$, yellow line), but is greatly reduced ($\Delta pH < 0.05$) and shifted to higher salinity (15-20) over a higher (but similar width) TA_f range approximately representative of the Mississippi River
20 (2115-2870 $\mu eq kg^{-1}$, solid black line; Table ??). Likewise, ΔpH is high ($\Delta pH > 0.1$) and at low S (4-5) for a lower TA_f range representative of the tropical Amazon River (246-549 $\mu eq kg^{-1}$, teal line; Table ??), and is reduced ($\Delta pH < 0.04$) over a similar TA_f range to the Amazon but shifted slightly higher to represent the Arctic Lena River (651-860 $\mu eq kg^{-1}$, black dash line; Table ??).

For our endmember mixing curves (Fig. ??) across an even larger range of mean TA_f (0-6000 $\mu eq kg^{-1}$), overall estuarine
25 pH sensitivity (ΔpH) to a given TA_f range (ΔTA_f) decreases (Fig. ??a) and salinity at maximum ΔpH increases (Fig. ??b) with increasing mean TA_f ($\overline{TA_f}$). While these dependencies are estimated using endmembers specific to the Fraser Strait of Georgia system, we propose that these relationships have broader implications for rivers and their neighboring estuaries. Specifically, mean river TA ($\overline{TA_f}$) primarily determines estuarine pH sensitivity (ΔpH and S at maximum ΔpH) to river TA variability (ΔTA_f). As such, low TA rivers like the Kennebec (yellow triangle right), Ob (white circle), and Yenisey (white
30 square, Fig. ??) may have larger seasonal ΔpH variations at lower salinities than high TA rivers like the Changjiang (black circle) and Mackenzie (white diamond), despite sharing similar ΔTA_f . Conversely, rivers with similar $\Delta TA_f : \overline{TA_f}$ ratios (e.g., Lena (white triangle up), Mackenzie (white diamond), Changiang (black circle), Mississippi (black diamond); Fig. ??a) may share similar ΔpH maxima as the increase in $\overline{TA_f}$ offsets the increase in ΔTA_f , but salinity at maximum ΔpH would still increase with $\overline{TA_f}$ independently of ΔTA_f (Fig. ??b).

Thus, for arbitrary rivers sharing the same Strait of Georgia seawater endmember, the estuaries of high TA rivers experience smaller seasonal estuarine pH ranges than those of low TA rivers over similar seasonal freshwater TA range widths. However, these high TA river estuaries also experience their zones of strongest seasonal pH sensitivity at higher salinities than their low TA counterparts, which likely impact a larger areal extent of the estuary (this zone is different than the zone of maximum pH sensitivity to changes in DIC alone which occurs at DIC~TA (Egleston et al., 2010)). In this regard, seasonal pH changes in the Strait of Georgia driven by mixing alone are large ($\Delta\text{pH} > 0.15$) because the Fraser (red star, Fig. ??a) is relatively low in TA but has a relatively high seasonal TA range relative to other world rivers. However, this large pH range is centered below salinity 10 so the impact on the estuary may not be as severe.

4.2 Comparison to other rivers and implications for future climate

Present-day carbonate chemistry in world rivers covers a large range (DIC or TA from ~ 50 to $7000 \mu\text{mol kg}^{-1}$; Fig. 8). Pollution drives part of this variability (black symbols, Fig. 8) as does latitude, in large part from the presence of carbonate rocks in many temperate drainage basins (Amiotte Suchet et al., 2003) – the tropical Amazon and Congo rivers have exceedingly low TA and DIC by contrast (cyan symbols, Fig. 8). Seasonal variability of DIC and TA far exceeds the Fraser in some rivers, particularly the polluted rivers but also the Yukon. However overall, the range of DIC:TA in most rivers is near or within the range determined for this study. The tropical rivers are an exception. The Congo River (cyan square, Fig. 8c and d), for example, has nearly constant DIC throughout the year while TA drops to less than half of the DIC concentration at peak river discharge (Wang et al., 2013). Another exception is glacial melt water (magenta square), which even at a DIC:TA more than twice as high as our High Carbon scenario, is $p\text{CO}_2$ -undersaturated relative to the atmosphere and continues to take up DIC as it mixes with seawater (Meire et al., 2015). Seasonal biological productivity may also play a strong role of regulating DIC in some temperate rivers by drawing down DIC, at least near the river mouth, as it does in the Fraser River. In the Columbia River estuary, DIC drawdown is strong in the spring, but is replaced by net heterotrophy during the summer and fall. This early transition to heterotrophy makes the Columbia estuary a net annual source of CO_2 to the atmosphere (Evans et al., 2013) despite maintaining a relatively low DIC:TA ratio (yellow square, Fig. 8). The Fraser estuary by contrast has a significantly higher DIC:TA ratio, but maintains a seasonally-persistent $p\text{CO}_2$ -undersaturation relative to the atmosphere because of strong productivity throughout most summers. the productive season occurs during high flow keeping DIC:TA low (pH high), while other rivers experience an increase in DIC:TA from low flow to high flow (Fig. 8c, d). The low flow DIC:TA ratio in the Fraser is thus uniquely high (Fig. 8c), although it is less able to exert influence on neighboring ocean waters due to a smaller river plume and storm-induced winter mixing. DIC and TA in most rivers are strongly flow (or seasonally) dependent, particularly the tropical rivers (Fig. 8).

In the coming decades, weathering rates and mean river TA are unlikely to change significantly due to climate (Riebe et al., 2001). In contrast, increasing atmospheric $p\text{CO}_2$ will increase DIC in the ocean and most likely in rivers as well. River DIC may be influenced by many additional variables, including changes in freshwater flow, human pressures (local anthropogenic inputs) and anticipated increases in river temperature. For example, the relatively high DIC:TA ratio of the present day glacial DIC and TA end-member yields a high DIC:TA ratio relative to most world rivers (magenta square, Fig. 8c, d), but is in equilibrium

with the atmosphere at a river temperature of 0°C (Meire et al., 2015), but if this pure glacier water were to experience a 10°C increase during its passage to the ocean, then outgassing would decrease river DIC by about 10% ($\sim 9 \mu\text{mol kg}^{-1}$) if ~~it~~ the melt water remained in atmospheric equilibrium. However, its pH would stay about the same (slight increase) in this scenario. More generally, ocean pH will become more sensitive to changes in dissolved CO₂ as the oceans become warmer and higher in overall CO₂ because of weakening buffer capacity (Hagens and Middelburg, 2016). Were this trend to be significant in the Strait of Georgia, it would further exacerbate the increased estuarine pH and Ω_A sensitivity that we observe at high river DIC in the biogeochemical model.

~~While the present study finds a maximum estuarine pH sensitivity to river TA at relatively low salinity (~ 10 for the Fraser Strait of Georgia endmembers, Fig. ??c), DIC changes to the system independent of TA generally impact estuarine pH most severely where DIC \sim TA ((Egleston et al., 2010), $S \sim 12-20$ for the Fraser Strait of Georgia), creating a salinity zone of particularly strong sensitivity (Hu and Cai, 2013). These future DIC increases will shift this zone to higher salinities. As the surface areas of various salinity zones in an estuary generally increase away from the river, this shift would increase the areal size of this highly sensitive zone at present-day river flows.~~

In addition to freshwater chemistry, the large seasonal freshwater flux from the Fraser River exerts a significant influence on estuarine pH, and particularly Ω_A , in the Strait of Georgia, with the highest flow years producing the most acidic and corrosive conditions. The Strait is relatively acidic in general throughout the water column compared to its primary conduit to the Pacific Ocean, the Juan de Fuca Strait, as well as the British Columbia continental shelf during upwelling (Ianson et al., 2016). The surface Strait of Georgia is also relatively acidic compared with oceanic extrapolations of fresh water endmembers from the otherwise similar, glacially-fed temperate Corcovado estuary in Chile (Torres et al., 2011), despite the higher extrapolated TA in the Fraser ~~having higher alkalinity than what~~ relative to the Corcovado estuary's primary freshwater source, the Puelo River ~~appears to have~~. This excess background DIC may contribute significantly to the persistent surface aragonite undersaturation observed (Ianson et al., 2016) and modeled (Moore-Maley et al., 2016) in the Strait during winter and during large summer freshets.

A warming climate has (Zhang et al., 2001) and will continue (Morrison et al., 2014) to reduce the peak freshet flows of glacial, temperate rivers and move the freshet timing earlier, which may reduce the severity of summer aragonite undersaturation in the Strait of Georgia associated with large freshets. Winter flows may also increase, however, which ~~may~~ could increase the sensitivity of the estuary to river chemistry during these low flow times beyond our model (currently insensitive) predictions. A changing freshet climatology may affect the significance of freshwater TA flow dependence as well. While many different studies consider flow dependent river TA to anticorrelate with discharge (e.g., Wang et al., 2013; Evans et al., 2013), the strong Fraser River TA hysteresis demonstrated by our data links the strongest Fraser River TA fluctuations to rapid pulses in river discharge. A future shift to smaller freshets will thus likely reduce the already weak influence of flow dependent freshwater TA in the model, supporting the use of fixed freshwater TA endmembers in large scale acidification projection models (e.g., Volta et al., 2016). However, the present study highlights the importance of choosing a freshwater TA endmember carefully. ~~In fact the surface Strait of Georgia is already aragonite-undersaturated for the whole winter season (Fig. ??g). Unsurprisingly, the river has the strongest impact during years with the highest river flows. These years have the lowest summer pH and Ω_A~~

when river carbonate chemistry remains constant (not shown, (Moore-Maley et al., 2016)). Thus as climate change continues to reduce peak flows, the impact of rivers on neighboring estuaries may decrease overall despite changing river carbonate chemistry.

5 Conclusions

5 The Fraser River is a large, free-flowing, glacially fed river that exerts a strong physical and chemical influence on a neighboring, semi-enclosed estuarine sea, the Strait of Georgia, that is DIC-rich relative to the open ocean. Based on recent data, we find that the Fraser River is moderately alkaline ($TA = 500\text{--}1000 \mu\text{mol kg}^{-1}$) but appears to carry a significant DIC load (high DIC:TA) even relative to many world rivers. TA appears to vary systematically with river flow, but does not display a simple dilution relationship. Rather it exhibits a strong hysteresis such that TA is a function of the change with respect to time in river
10 flow.

We examined the sensitivity of Ω_A and pH in the Strait of Georgia to Fraser River carbonate chemistry by summarizing the results of a coupled biogeochemical model across 12 hydrological cycles and 18 freshwater TA and DIC:TA combinations. Model results show that estuarine pH and Ω_A are strongly sensitive to river flow and river carbonate chemistry at moderate to low model salinities (< 20), and generally decrease as river flow or river DIC increases. The primary reason for this sensitivity
15 is the strong estuarine DIC regulation achieved both by physical river shading effects on primary productivity, and by the DIC contribution relative to TA from the freshwater endmember to the estuary.

Model DIC and pH are tightly coupled by the dominant influence of the carbonate equilibrium, however estuarine Ω_A responds asynchronously from DIC and pH to increasing freshwater TA at low and moderate freshwater DIC:TA (which we consider to represent past and present) scenarios as river DIC:TA approaches unity. Under these conditions the carbonate ion
20 follows DIC and simple dilution/enhancement controls Ω_A . This estuarine Ω_A response reverses when freshwater DIC:TA becomes larger ($> \sim 1.1$) because the carbonate ion makes up an increasingly smaller portion of the total DIC and the Ω_A dynamics are thus no longer controlled by physical dilution. In our highest freshwater DIC:TA scenario, Ω_A responds to estuarine DIC:TA similarly to pH.

The Fraser river estuary is biological productive, which modulates its sensitivity to river chemistry. In winter, productivity is
25 low so estuary chemistry nearly follows simple endmember mixing theory. Once the seasonal phytoplankton bloom occurs and there is significant biological drawdown of DIC, both estuarine pH and Ω_A increase markedly away from the physical mixing line. Thus, even though the river flow is at a maximum during summer, estuarine sensitivity to river chemistry (in particular to DIC) is significantly reduced. Finally, the strong impact of Fraser River flow input on pH and Ω_A in the Strait of Georgia will be reduced as the Fraser watershed makes its expected transition to smaller, earlier freshets with climate change. However,
30 if DIC:TA ratios increase in one or both of the river-ocean endmembers as anticipated with rising atmospheric CO_2 , then the increased sensitivity of estuarine pH and Ω_A associated with this endmember change may counteract the flow regime changes to some degree.

The Fraser River is moderately alkaline ($TA = 500\text{--}1350\ \mu\text{mol kg}^{-1}$) due to chemical weathering, however, its DIC:TA ratio is high, during winter (low flow) even relative to rivers that are considered heavily polluted. While it contributes less freshwater and TA to the Northeast Pacific ocean than does the Columbia River, it exerts strong influence over a large, semi-enclosed estuarine region that is vulnerable to climate change and DIC-rich relative to the open ocean. We assessed recent and historic observations of the carbonate system in the river and its estuary, the southern Strait of Georgia. We then investigated the sensitivity of surface estuarine pH and Ω_A to river TA and pH (18 scenarios) using a predictive biogeochemical model over more than a decade of present-day physical forcing scenarios with strong interannual variability.

Estimated freshwater TA endmembers extrapolated from Strait of Georgia cruise data and Fraser River TA observations near the mouth decrease with increasing river flow, as is the case in most temperate rivers. However, pH is highest during peak flow despite this low alkalinity and significant summer warming, likely due to biological uptake of DIC. This seasonal variation means that, unlike some other rivers (e.g., Congo), the Fraser River is most acidic (high DIC:TA) during low flow when river impact on the estuary is at a minimum. The Fraser is always well undersaturated with respect to aragonite ($\Omega_A \leq 0.1$), typical of the more acidic Arctic and tropical rivers.

Within the Fraser's Strait of Georgia estuary, including our model site (~ 25 km seaward of the river mouth), the river plays a key role in driving strong seasonal cycles in physical and biogeochemical variables. For roughly three months during summer, surface salinity is low and variable, ranging from 5–20, depending on strength and timing of the Fraser freshet. In contrast, winter conditions in the estuary are less variable and more saline, typically near 25 (always < 30). Like in the Fraser, surface pH in the Strait of Georgia is high during the summer freshet (8.1–8.35) when biological productivity throughout the Strait is also high, as is typical of temperate systems. This summer estuarine pH is sensitive to both river TA and DIC:TA ratio (pH), but large DIC fluxes associated with the summer productivity reduces the sensitivity to the latter. Winter estuarine pH is always around 8.0 and relatively insensitive to river TA and DIC:TA ratio since river flow is at a minimum.

During freshets when salinity is low (< 20) in neighboring estuaries, surface Ω_A becomes decoupled from pH due to the impact of calcium and carbonate ion dilution. Thus, despite high productivity in the southern Strait of Georgia (high pH) during summer, there are long periods (up to 40 days) of surface Ω_A undersaturation during strong freshets, which occur in nearly half of the years studied. These periods occur regardless of river carbonate chemistry, excepting the single highest freshwater TA and pH scenario, which represents only the strongly alkaline rivers at present day like the Mississippi, Changjiang, and Mackenzie. The duration of these undersaturated periods is less sensitive to river TA at high river DIC:TA (low pH) than is estuarine pH. However, low river DIC:TA (high pH) allows river TA to exert more control, decreasing this duration and even its incidence, as may have been the case in many estuaries, including the Fraser, in the past.

While the sensitivity of estuarine pH to changes in river TA is low for alkaline (high TA) rivers, the salinity zone of this sensitivity is high and potentially covers large areal extents. Conversely, the greater sensitivity of estuarine pH for low TA rivers is maximized at low salinities and thus may be confined to smaller sections of the estuary. However, in the future as atmospheric CO_2 continues to dissolve into aquatic systems, estuarine pH sensitivity to river TA will increase in the estuaries of moderately alkaline rivers like the Fraser because of rising DIC:TA. These DIC:TA increases may also reduce the ability of rivers like the Fraser to buffer against estuarine surface aragonite undersaturation. Additionally, like the zones of maximum

estuarine pH sensitivity to freshwater TA, the zones of maximum estuarine pH sensitivity to DIC changes (DIC~TA) will be pushed to higher salinities as well, likely affecting larger areal extents of estuaries, depending on changes in river flow.

5 *Code and data availability.* Model source code and run scripts are available from the UBC Salish Sea bitbucket repository <https://bitbucket.org/account/user/salishsea/projects/SOG>. Results files for the sensitivity experiments will be hosted at the Abacus Dataverse Network which is a research data repository of the British Columbia Research Libraries' Data Services <http://dvn.library.ubc.ca/dvn>, prior to publication. Model initialization data is available from the Fisheries and Oceans Canada Institute of Ocean Sciences Data Archive <http://www.pac.dfo-mpo.gc.ca/science/oceans/data-donnees/search-recherche/profiles-eng.asp>. Carbon cruise data from the Fraser River plume presented in Ianson et al. (2016) and additional new observations from two field campaigns will be hosted at the U.S. Department of Energy's ESS-DIVE data repository prior to publication. All other data presented in this article are available from their cited URL locations.

10 *Competing interests.* The authors declare that they have no conflict of interest.

15 *Acknowledgements.* This work was supported by a Natural Sciences and Engineering Research Council of Canada (NSERC) Discovery grant to the third author, Fisheries and Oceans Canada's Climate Change Science Initiative and International Governance Strategy programs, and the Marine Environmental Observation, Prediction, and Response (MEOPAR) Network of Centres of Excellence of Canada. We thank Diane Masson and Peter Chandler (IOS) for sharing their Strait of Georgia survey data, and Eleanor Simpson and Karen Kohfeld (Simon Fraser University), Marty Davelaar (IOS), Yves Perrault (Little Wing Oysters) and Andre Comeau (Okeover Organic Oysters) for collecting and sharing data from the Freke Ancho River. We thank Doug Latornell at UBC for developing the model working environment, and Robie Macdonald and Paul Covert for providing helpful insights. The second author thanks Niki Gruber for his hospitality at ETH-Zurich while this manuscript was completed. We also acknowledge five anonymous reviewers for their detailed feedback.

References

- Allen, S., D., L., Olson, E., and Pawlowicz, R.: Timing of the spring phytoplankton bloom in the Strait of Georgia, 2015 and 2016., in: State of the physical, biological and selected fishery resources of Pacific Canadian marine ecosystems in 2015., edited by Chandler, P., King, S., and Perry, I., vol. 3179, pp. 147–152, Can. Tech. Rep. Fish. Aquat. Sci., Canada, 2016.
- 5 Allen, S. E. and Wolfe, M. A.: Hindcast of the timing of the spring phytoplankton bloom in the Strait of Georgia, 1968-2010, *Prog. Oceanogr.*, 115, 6–13, doi:10.1016/j.pocean.2013.05.026, 2013.
- Amiotte Suchet, P., Probst, J., and Ludwig, W.: Worldwide distribution of continental rock lithology: Implications for the atmospheric/soil CO₂ uptake by continental weathering and alkalinity river transport to the oceans, *Glob. Biogeochem. Cycles*, 17, 1038, doi:10.1029/2002GB001891, 2003.
- 10 Bianucci, L., Denman, K. L., and Ianson, D.: Low oxygen and high inorganic carbon on the Vancouver Island Shelf, *J. Geophys. Res. Oceans*, 116, C07011, doi:10.1029/2010JC006720, 2011.
- Cai, W.: Riverine inorganic carbon flux and rate of biological uptake in the Mississippi River plume, *Geophys. Res. Lett.*, 30, 1032, doi:10.1029/2002GL016312, 2003.
- Cai, W., Wang, Y., and Hodson, R. E.: Acid-base properties of dissolved organic matter in the estuarine waters of Georgia, USA, *Geochim. Cosmochim. Ac.*, 62, 473–483, doi:10.1016/S0016-7037(97)00363-3, 1998.
- 15 Cai, W., Hu, X., Huang, W., Murrell, M. C., Lehrter, J. C., Lohrenz, S. E., Chou, W., Zhai, W., Hollibaugh, J. T., Wang, Y., Zhao, P., Guo, X., Gundersen, K., Dai, M., and Gong, G.: Acidification of subsurface coastal waters enhanced by eutrophication, *Nature Geosci.*, 4, 766–770, doi:10.1038/ngeo1297, 2011.
- Cai, W.-J., Huang, W.-J., Luther, G. W., Pierrot, D., Li, M., Testa, J., Xue, M., Joesoef, A., Mann, R., Brodeur, J., Xu, Y.-Y., Chen, B., 20 Hussain, N., Waldbusser, G. G., Cornwell, J., and Kemp, W. M.: Redox reactions and weak buffering capacity lead to acidification in the Chesapeake Bay, *Nature Communications*, 8, doi:doi:10.1038/s41467-017-00417-7, 2017.
- Cameron, E. M. and Hattori, K.: Strontium and neodymium isotope ratios in the Fraser River, British Columbia: a riverine transect across the Cordilleran orogen, *Chem. Geol.*, 137, 243–253, doi:10.1016/S0009-2541(96)00168-4, 1997.
- Cloern, J. E., Foster, S. Q., and Kleckner, A. E.: Phytoplankton primary production in the world's estuarine-coastal ecosystems, *Biogeosci.*, 25 11, 2477–2501, doi:10.5194/bg-11-2477-2014, 2014.
- Cloern, J. E., Abreu, P. C., Carstensen, J., Chauvaud, L., Elmgren, R., Grall, J., Greening, H., Johansson, J. O. R., Kahru, M., Sherwood, E. T., Xu, J., and Yin, K.: Human activities and climate variability drive fast-paced change across the world's estuarine-coastal ecosystems, *Glob. Change Biol.*, 22, 513–529, doi:10.1111/gcb.13059, 2015.
- Collins, A. K., Allen, S. E., and Pawlowicz, R.: The role of wind in determining the timing of the spring bloom in the Strait of Georgia, *Can. J. Fish. Aquat. Sci.*, 66, 1597–1616, doi:10.1139/F09-071, 2009.
- 30 Covington, A. K., Whalley, P. D., and Davison, W.: Procedures for the measurement of pH in low ionic strength solutions including fresh-water, *Analyst*, 108, 1528–1532, doi:10.1039/AN9830801528, 1983.
- de Fátima F. L. Rasera, M., Krusche, A. V., E.Richey, J., Ballester, M. V. R., and Victória, R. L.: Spatial and temporal variability of pCO₂ and CO₂ efflux in seven Amazonian rivers, *Biogeochemistry*, 116, 241–259, doi:10.1007/s10533-013-9854-0, 2013.
- 35 de Mora, S. J.: The distribution of alkalinity and pH in the Fraser Estuary, *Environ. Technol. Lett.*, 4, 35–46, doi:10.1080/09593338309384169, 1983.

- Dickson, A. G., Sabine, C. L., and Christian, J. R.: Guide to Best Practices for Ocean CO₂ Measurements, PICES Special Publication 3, cdiac.ornl.gov/oceans/Handbook_2007.html, 2007.
- Egleston, E. S., Sabine, C. L., and Morel, F. M. M.: Revelle revisited: Buffer factors that quantify the response of ocean chemistry to changes in DIC and alkalinity, *Glob. Biogeochem. Cycles*, 24, GB1002, doi:10.1029/2008GB003407, 2010.
- 5 Ethier, A. and Bedard, J.: Development of a real-time water quality buoy for the Fraser River Estuary, AXYS Technologies Inc., Sidney, British Columbia, 2007.
- Evans, W., Hales, B., and Strutton, P. G.: *p*CO₂ distributions and air-water CO₂ fluxes in the Columbia River estuary, *Estuar. Coast. Shelf Sci.*, 117, 260–272, doi:10.1016/j.ecss.2012.12.003, 2013.
- Fennel, K., Hu, J., Laurent, A., Marta-Almeida, M., and Hetland, R.: Sensitivity of hypoxia predictions for the northern Gulf of Mexico to sediment oxygen consumption and model nesting, *J. Geophys. Res. Oceans*, 118, 990–1002, doi:10.1002/jgrc.20077, 2013.
- Frankignoulle, M., Bourge, I., and Wollast, R.: Atmospheric CO₂ fluxes in a highly polluted estuary (the Scheldt), *Limnol. Oceanogr.*, 41, 365–369, doi:10.4319/lo.1996.41.2.0365, 1996.
- Hagens, M. and Middelburg, J. J.: Generalised expressions for the response of pH to changes in ocean chemistry, *Geochimica et Cosmochimica Acta*, 187, 334 – 349, doi:<https://doi.org/10.1016/j.gca.2016.04.012>, 2016.
- 15 Haigh, R., Ianson, D., Holt, C. A., Neate, H. E., and Edwards, A. M.: Effects of ocean acidification on temperate coastal marine ecosystems and fisheries in the Northeast Pacific, *PLoS ONE*, 10, e0117533, doi:doi:10.1371/journal.pone.0117533, 2015.
- Harrison, P. J., Fulton, J. D., Taylor, F. J. R., and Parsons, T. R.: Review of the biological oceanography of the Strait of Georgia: pelagic environment, *Can. J. Fish. Aquat. Sci.*, 40, 1064–1094, doi:10.1139/f83-129, 1983.
- Hellings, L., Dehairs, F., Damme, S. V., and Baeyens, W.: Dissolved inorganic carbon in a highly polluted estuary (the Scheldt), *Limnol. Oceanogr.*, 46, 1406–1414, doi:10.4319/lo.2001.46.6.1406, 2001.
- 20 Hernández-Ayón, J. M., Zirino, A., Dickson, A. G., Camiro-Vargas, T., and Valenzuela-Espinoza, E.: Estimating the contribution of organic bases from microalgae to the titration alkalinity in coastal seawaters, *Limnol. Oceanogr. Methods*, 5, 225–232, doi:10.4319/lom.2007.5.225, 2007.
- Hofmann, A. F., Middleburg, J. J., Soetaert, K., and Meysman, F. J. R.: pH modelling in aquatic systems with time-variable acid-base dissociation constants applied to the turbid, tidal Scheldt estuary, *Biogeosci.*, 6, 1539–1561, doi:10.5194/bg-6-1539-2009, 2009.
- 25 Hu, X. and Cai, W.: Estuarine acidification and minimum buffer zone — A conceptual study, *Geophys. Res. Lett.*, 40, 5176–5181, doi:10.1002/grl.51000, 2013.
- Hunt, C. W., Salisbury, J. E., and Vandemark, D.: Contribution of non-carbonate anions to total alkalinity and overestimation of *p*CO₂ in New England and New Brunswick rivers, *Biogeosci.*, 8, 3069–3076, doi:10.5194/bg-8-3069-2011, 2011.
- 30 Hunt, C. W., Salisbury, J. E., and Vandemark, D.: CO₂ input dynamics and air-sea exchange in a large New England estuary, *Estuar. Coast.*, 37, 1078–1091, doi:10.1007/s12237-013-9749-2, 2014.
- Ianson, D., Allen, S. E., Moore-Maley, B. L., Johannessen, S. C., and Macdonald, R. W.: Vulnerability of a semi-enclosed estuarine sea to ocean acidification in contrast with hypoxia, *Geophys. Res. Lett.*, 43, 5793–5801, doi:10.1002/2016GL068996, 2016.
- Jiang, L., Feely, R. A., Carter, B. R., Greeley, D. J., Gledhill, D. K., and Arzayus, K. M.: Climatological distribution of aragonite saturation state in the global oceans, *Glob. Biogeochem. Cycles*, 29, 1656–1673, doi:10.1002/2015GB005198, 2015.
- 35 Kennedy, V. C.: Mineralogy and cation-exchange capacity of sediments from selected streams, Prof. Paper 433-D, U.S. Geol. Surv., 1965.
- Kim, H. and Lee, K.: Significant contribution of dissolved organic matter to seawater alkalinity, *Geophys. Res. Lett.*, 36, L20603, doi:10.1029/2009GL040271, 2009.

- Koeve, W. and Oschlies, A.: Potential impact of DOM accumulation on $f\text{CO}_2$ and carbonate ion computations in ocean acidification experiments, *Biogeosci.*, 9, 3787–3798, doi:10.5194/bg-9-3787-2012, 2012.
- Large, W. G., McWilliams, J. C., and Doney, S. C.: Oceanic vertical mixing: a review and a model with a nonlocal boundary layer parametrization, *Rev. Geophys.*, 32, 363–403, doi:10.1029/94RG01872, 1994.
- 5 LeBlond, P. H.: The Strait of Georgia: functional anatomy of a coastal sea, *Can. J. Fish. Aquat. Sci.*, 40, 1033–1063, doi:10.1139/f83-128, 1983.
- Lewis, E. R. and Wallace, D. W. R.: Program Developed for CO_2 System Calculations, DOE (U.S. Department of Energy), ORNL/CDIAC-105, 1998.
- Masson, D.: Seasonal water mass analysis for the Straits of Juan de Fuca and Georgia, *Atmos. Ocean*, 44, 1–15, doi:10.3137/ao.440101, 10 2006.
- Masson, D. and Peña, A.: Chlorophyll distribution in a temperate estuary: The Strait of Georgia and Juan de Fuca Strait, *Estuarine Coastal Shelf Sci.*, 82, 19–28, doi:10.1016/j.ecss.2008.12.022, 2009.
- Meire, L., Søggaard, D. H., Mortensen, J., Meysman, R. J. R., Soetaert, K., Arendt, K. E., Juul-Pedersen, T., Blicher, M. E., and Rysgaard, S.: Glacial meltwater and primary production are drivers of strong CO_2 uptake in fjord and coastal waters adjacent to the Greenland Ice 15 Sheet, *Biogeosciences*, 12, 2347–2363, 2015.
- Meybeck, M.: Global chemical weathering of surficial rocks estimated from river dissolved loads, *Am. J. Sci.*, 287, 401–428, doi:10.2475/ajs.287.5.401, 1987.
- Millero, F. J.: Carbonate constants for estuarine waters, *Mar. Fresh. Res.*, 61, 139–142, doi:10.1071/MF09254, 2010.
- Mook, W. G. and Koene, B. K. S.: Chemistry of dissolved inorganic carbon in estuarine and coastal brackish waters, *Estuar. Coast. Mar. Sci.*, 20 3, 325–336, doi:10.1016/0302-3524(75)90032-8, 1975.
- Moore-Maley, B. L., Allen, S. E., and Ianson, D.: Locally-driven interannual variability of near-surface pH and Ω_A in the Strait of Georgia, *J. Geophys. Res. Oceans*, 121, 1600–1625, doi:10.1002/2015JC011118, 2016.
- Morrison, J., Callendar, W., Foreman, M. G. G., Masson, D., and Fine, I.: A model simulation of future oceanic conditions along the British Columbia continental shelf. Part I: Forcing fields and initial conditions, *Atmos. Ocean*, 52, 1–19, doi:10.1080/07055900.2013.868340, 25 2014.
- Nightingale, P. D., Malin, G., Law, C. S., Watson, A. J., Liss, P. S., Liddicoat, M. I., Boutin, J., and Upstill-Goddard, R. C.: In situ evaluation of air-sea gas exchange parametrizations using novel conservative and volatile tracers, *Global Biogeochem. Cycles*, 14, 373–387, doi:10.1029/1999GB900091, 2000.
- Pawlowicz, R., Riche, O., and Halverson, M.: The circulation and residence time of the Strait of Georgia using a simple mixing-box approach, 30 *Atmos. Ocean*, 45, 173–193, doi:10.3137/ao.450401, 2007.
- Peña, A., Masson, D., and Callendar, W.: Annual plankton dynamics in a coupled physical-biological model of the Strait of Georgia, British Columbia, *Prog. Oceanogr.*, 146, 58–74, doi:10.1016/j.pocean.2016.06.002, 2016.
- Preston-Thomas, H.: The international temperature scale of 1990 (ITS-90), *Metrologia*, 27, 3–10, doi:10.1088/0026-1394/27/1/002, 1990.
- Riche, O.: Time-dependent inverse box-model for the estuarine circulation and primary productivity in the Strait of Georgia, Ph.D. thesis, 35 University of British Columbia, 2011.
- Richey, J. E., Hedges, J. I., Devol, A. H., Quay, P. D., Victoria, R., Martinelli, L., and Forsberg, B. R.: Biogeochemistry of carbon in the Amazon River, *Limnol. Oceanogr.*, 35, 352–371, doi:10.4319/lo.1990.35.2.0352, 1990.

- Riebe, C. S., Kirchner, J. W., Granger, D. E., and Finkel, R. C.: Strong tectonic and weak climatic control of long-term chemical weathering rates, *Geol.*, 29, 511–514, doi:10.1130/0091-7613(2001)029<0511:STAWCC>2.0.CO;2, 2001.
- Riley, J. P. and Tongudai, M.: The major cation/chlorinity ratios in sea water, *Chem. Geol.*, 2, 263–269, doi:10.1016/0009-2541(67)90026-5, 1967.
- 5 Roegner, G. C., Seaton, C., and Baptista, A. M.: Climatic and tidal forcing of hydrography and chlorophyll concentrations in the Columbia River Estuary, *Estuar. Coast.*, 34, 281–296, doi:10.1007/s12237-010-9340-z, 2011.
- Salisbury, J., Green, M., Hunt, C., and Campbell, J.: Coastal acidification by rivers: a threat to shellfish?, *Eos Trans. AGU*, 89, 513, doi:10.1029/2008EO500001, 2008.
- Sarmiento, J. L. and Gruber, N.: *Ocean Biogeochemical Dynamics*, Princeton University Press, 2006.
- 10 Schindler, D. W.: Effects of acid rain on freshwater ecosystems, *Science*, 239, 149–157, doi:10.1126/science.239.4836.149, 1988.
- Torres, R., Pantoja, S., Harada, N., González, H. E., Daneri, G., Frangopulos, M., Rutllant, J. A., Duarte, C. M., Rúaiz-Halpern, S., Mayol, E., and Fukasawa, M.: Air-sea CO₂ fluxes along the coast of Chile: From CO₂ outgassing in central northern upwelling waters to CO₂ uptake in southern Patagonian fjords, *Journal of Geophysical Research: Oceans*, 116, doi:10.1029/2010JC006344, <http://dx.doi.org/10.1029/2010JC006344>, c09006, 2011.
- 15 UNESCO: The Practical Salinity Scale 1978 and the International Equation of State of Seawater 1980, Tech. rep., UNESCO technical papers in marine science No. 36, 1981.
- Volta, C., Laruelle, G. G., Arndt, S., and Regnier, P.: Linking biogeochemistry to hydro-geometrical variability in tidal estuaries: a generic modeling approach, *Hydrol. Earth Syst. Sci.*, 20, 991–1030, doi:10.5194/hess-20-991-2016, 2016.
- Voss, B. M., Peucker-Ehrenbrink, B., Eglinton, T. I., Fiske, G., Wang, Z. A., Hoering, K. A., Montluçon, D. B., LeCroy, C., Pal, S., Marsh, S., Gillies, S. L., Janmaat, A., Bennett, M., Downey, B., Fanslau, J., Fraser, H., Macklam-Harron, G., Martinec, M., and Wiebe, B.: Tracing river chemistry in space and time: dissolved inorganic constituents of the Fraser River, Canada, *Geochim. Cosmochim. Ac.*, 124, 283–308, doi:10.1016/j.gca.2013.09.006, 2014.
- Waldbusser, G. G. and Salisbury, J. E.: Ocean acidification in the coastal zone from an organism's perspective: multiple system parameters, frequency domains, and habitats, *Ann. Rev. Mar. Sci.*, 6, 221–247, doi:10.1146/annurev-marine-121211-172238, 2014.
- 25 Waldbusser, G. G., Hales, B., Langdon, C. J., Haley, B. A., Schrader, P., Brunner, E. L., Gray, M. W., Miller, C. A., and Gimenez, I.: Saturation-state sensitivity of marine bivalve larvae to ocean acidification, *Nat. Clim. Change*, 5, 273–280, doi:10.1038/nclimate2479, 2015.
- Wang, Z. A., Bienvenu, D. J., Mann, P. J., Hoering, K. A., Poulsen, J. R., Spencer, R. G. M., and Holmes, R. M.: Inorganic carbon speciation and fluxes in the Congo River, *Geophys. Res. Lett.*, 40, 511–516, doi:10.1002/grl.50160, 2013.
- 30 Wanninkhof, R.: Relationship between wind speed and gas exchange over the ocean, *J. Geophys. Res.*, 97, 7373–7382, doi:10.1029/92JC00188, 1992.
- Weiss, R. F.: Carbon dioxide in water and seawater: the solubility of a non-ideal gas, *Mar. Chem.*, 2, 203–215, doi:10.1016/0304-4203(74)90015-2, 1974.
- Wheeler, J. O., Brookfield, A. J., Gabrielse, H., Monger, J. W. H., Tipper, H. W., and Woodsworth, G. J.: Terrane map of the Canadian Cordillera, Map 1713A, *Geol. Surv. Can.*, scale 1:200,000, 1991.
- 35 Whitfield, M. and Turner, D. R.: The carbon dioxide system in estuaries - an inorganic perspective, *Sci. Total Environ.*, 49, 235–255, doi:10.1016/0048-9697(86)90243-3, 1986.

Xue, L., Cai, W.-J., Sutton, A. J., and Sabine, C.: Sea surface aragonite saturation state variations and control mechanisms at the Gray's Reef time-series site off Georgia, USA (2006-2007), *Marine Chemistry*, 195, 27 – 40, doi:<https://doi.org/10.1016/j.marchem.2017.05.009>, 2017.

5 Zhai, W., Dai, M., and Guo, X.: Carbonate system and CO₂ degassing fluxes in the inner estuary of Changjiang (Yangtze) River, China, *Mar. Chem.*, 107, 342–356, doi:<http://dx.doi.org/10.1016/j.marchem.2007.02.011>, 2007.

Zhang, X., Havery, K. D., Hogg, W. D., and Yuzyk, T. R.: Trends in Canadian Streamflow, *Water Resources Res.*, 37, 987–998, doi:[10.1029/2000WR900357](https://doi.org/10.1029/2000WR900357), 2001.

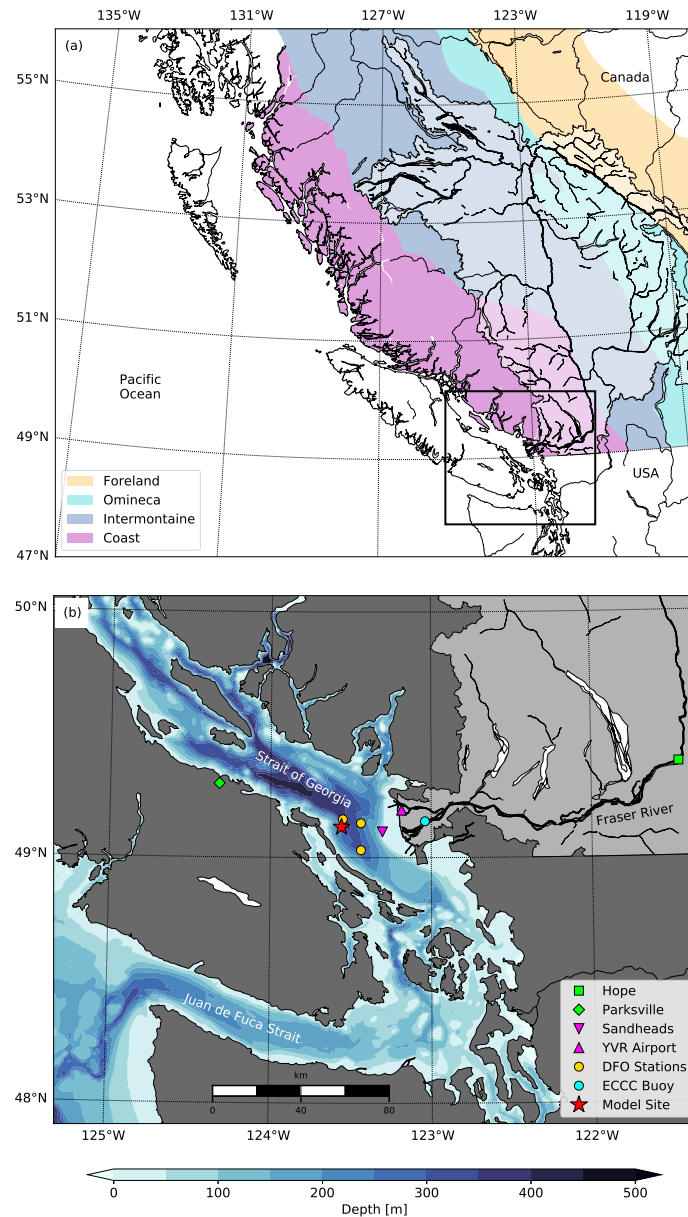


Figure 1. Maps of (a) the Fraser River watershed **with** showing the major geologic belts (Wheeler et al., 1991), and (b) the lower Fraser River **delta** and Strait of Georgia showing the model location (red star), **with** Environment and Climate Change Canada (ECCC) **carbon chemistry sampling sites (2-4) in green**, ECCC meteorological (Sandheads and YVR, magenta symbols) **stations (5-6)** and river gauging (Fraser River at Hope and Englishman River at Parkville, green symbols) stations used to force the model, and Fisheries and Oceans Canada (DFO) sampling stations (yellow circles) and (4, 7) in yellow, and the model location (1) in red. TA measurements (2-4) and pH readings at the ECCC Fraser River Water Quality Buoy (cyan circle) (3) are used to constrain Fraser River TA and pH, respectively. **carbon chemistry (Table ??)**. The model is forced with hourly windspeed (6) and meteorological (5) observations (<http://climate.weather.gc.ca/>), and daily Fraser (4) and Englishman (7) River discharge (<http://wateroffice.ec.gc.ca/>).

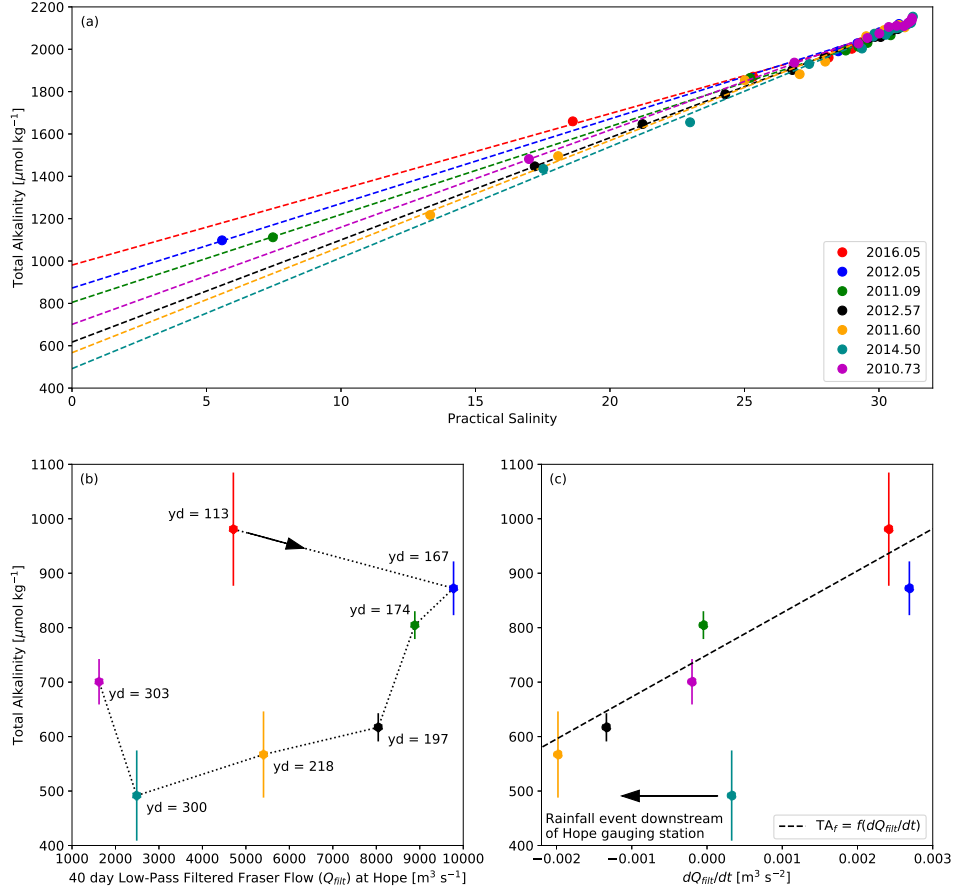


Figure 2. (a) Observed TA versus salinity (S) (circles) and linear regressions (dashed lines) from several 7 Department of Fisheries and Oceans Canada (DFO) Strait of Georgia cruises near in the Fraser River plume prior to 1980 (de Mora, 1983) and post-2009 ((Ianson et al., 2016), Table S1), (b) TA extrapolated to $S = 0$ versus low-pass filtered (40-day cutoff) Fraser River discharge (Q_{fit}) at Hope (circles) plotted in sequence of yearday (yd) as indicated by the dashed line and labels, and (c) TA extrapolated to $S = 0$ versus Q_{fit}/dt (circles) with the flow dependent freshwater TA parameterization used in this study (Eq. 1) overplotted (dashed line). Cruise ID numbers (legend) begin with the sampling year. Each cruise contains at least one datapoint at $S < 20$. Errorbars (b and c) are the 95% confidence intervals associated with the extrapolation to $S = 0$ using linear regression (a). TA is generally conservative with S except near $S = 0$ (de Mora, 1983) – observations where $S < 0.1$ are excluded from the regressions. Extrapolated TA values to $S = 0$ are used as freshwater TA endmember estimates (Table ??).

Figure 2. Fraser River TA (a) extrapolated endmembers, (b) observations (ECCC) near the river mouth, and (c) observations (ECCC) at Hope, BC, and (d) ECCC buoy pH observations (Table ??) all versus Fraser River discharge near the mouth estimated (Pawlowicz et al., 2007) from flow observations at the Hope ECCC flow gauge (<http://www.wateroffice.ec.gc.ca/>; Fig. 1a). Solid symbols (a) are the observed TA at $S=0$, where available, from the corresponding open symbol cruise extrapolations. Cruise numbers (a) are the same as in Fig. ?? and correspond to (de Mora, 1983) prior to 1980 and (Ianson et al., 2016) post 2010. The fits shown are least-squares regressions where $Q_n = Q/1000 \text{ m}^3 \text{ s}^{-1}$, Q being the estimated discharge near the river mouth. The regressions are used to define flow-dependent TA scenarios for testing model pH and Ω_A sensitivity.

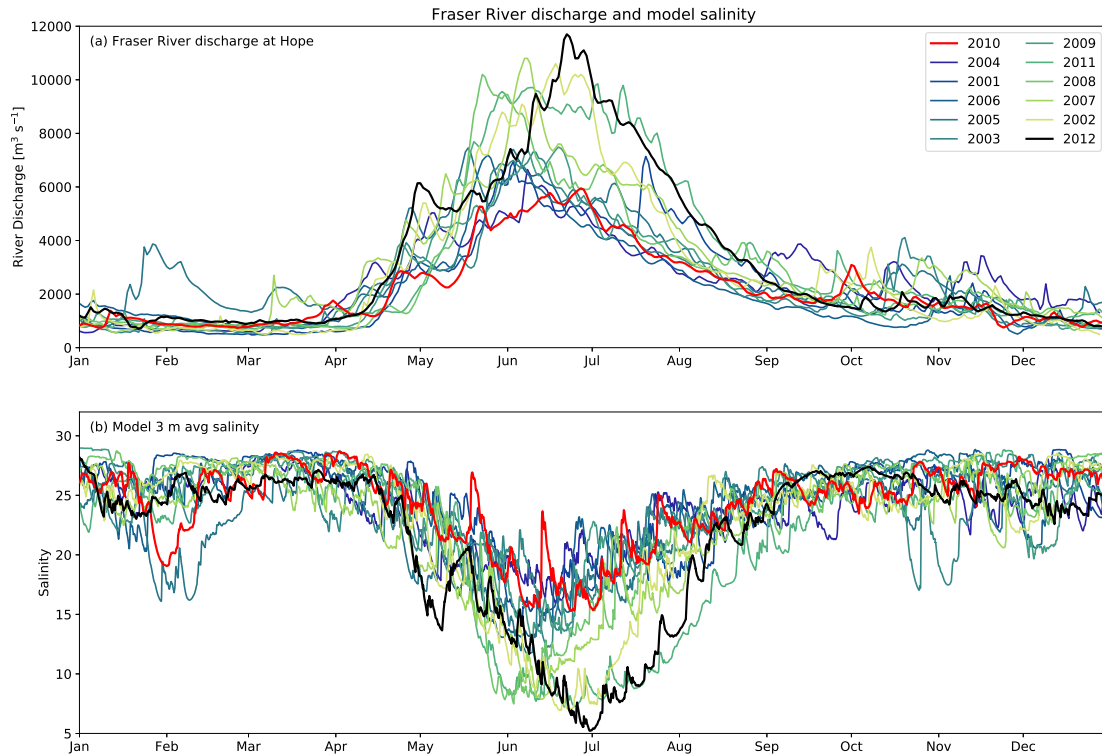


Figure 3. (a) Fraser River discharge at Hope versus yearday and (b) model top 3 m averaged salinity shown for each year in the 12 year period considered in this study. The Fraser River flow regime is characterized by a prominent summer freshet associated with summer glacial melt and smaller rainfall-dominated winter spikes. Model salinity reflects this overall pattern. Individual years are plotted in order of increasing freshet (peak) size. The smallest (2010) and largest (2012) flow years are highlighted in red and black, respectively.

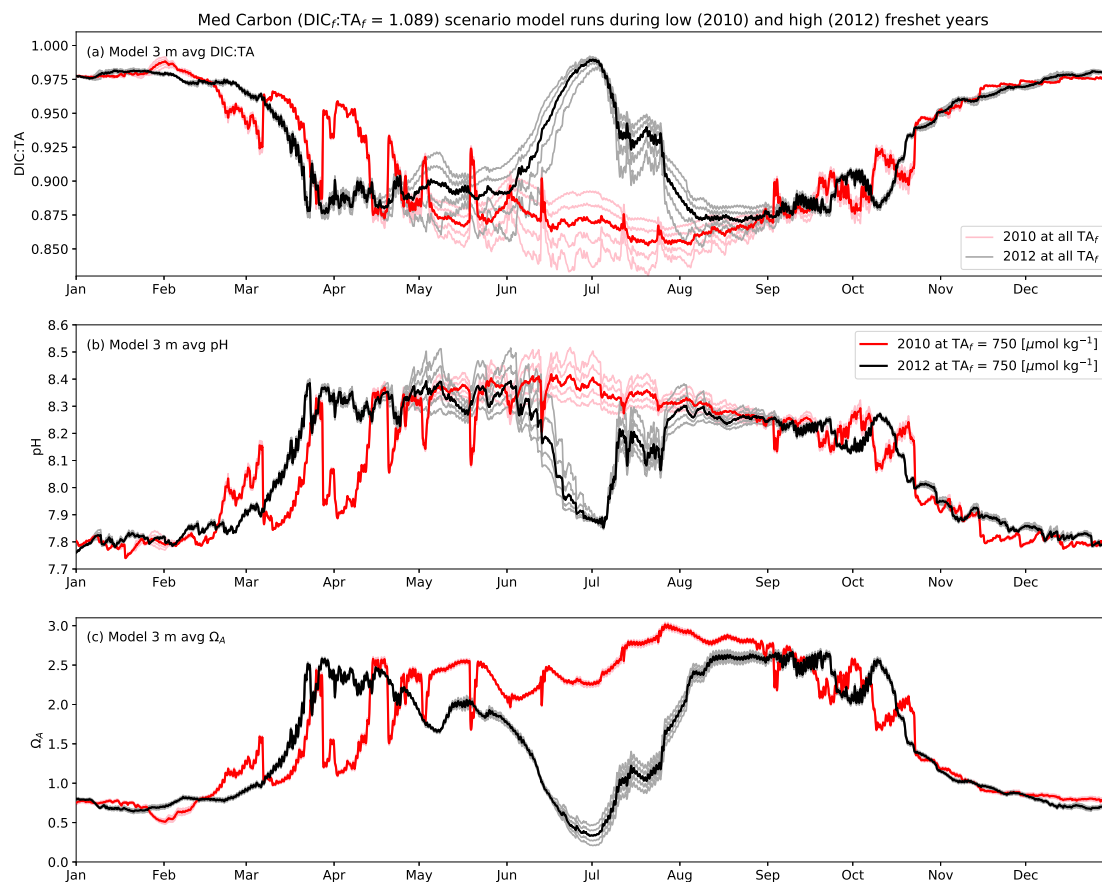


Figure 4. Timeseries of model top 3 m averaged (a) DIC:TA, (b) pH, and (c) Ω_A for all TA scenarios (Table 2) during 2010 (red/pink curves) and 2012 (black/gray) curves under the Med Carbon scenario ($DIC_f:TA_f = 1.089$), colors consistent with Fig. 3. The bold curves show model results at $TA_f = 750 \mu\text{mol kg}^{-1}$ and the lighter curves show model results at all TA_f . All 3 quantities demonstrate a seasonal cycle consistent with biologically-driven DIC decreases in summer, increases in winter, and variations in spring associated with the spring bloom season. A strong mid-summer DIC increase is present in the 2012 results when river discharge is strong but absent in the 2010 results when river discharge is weaker.

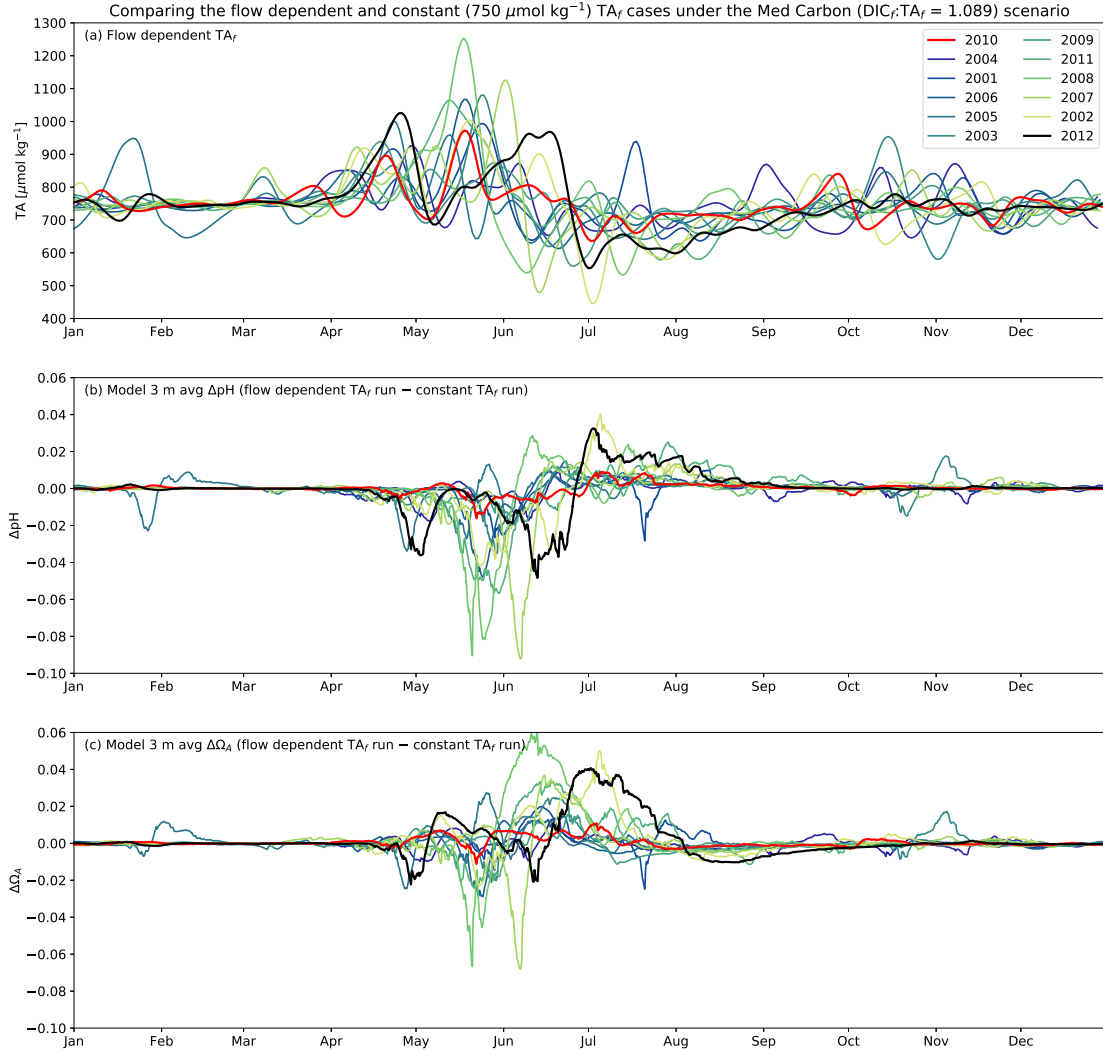


Figure 5. Results of the flow dependent TA_f case for each year in the 12 year record: (a) The flow dependent TA_f parameterization (Eq. 1), and (b and c) differences between flow dependent and constant ($750 \mu\text{mol kg}^{-1}$) TA_f runs at $(\text{DIC}:\text{TA})_f = 1.089$ for (b) 3 m averaged pH and (c) 3 m averaged Ω_A . Years of record are plotted in order of increasing freshet size with the lowest (2010) and highest (2012) years highlighted in red and black, as in Fig. 3. Since flow dependence is proportional to dQ_{fitt}/dt , the strongest effects surround the freshet generally with pH and Ω_A decreases prior to and increases after the freshet.

Summary of all model runs (3 m avg) averaged over salinity < 20 (summer)

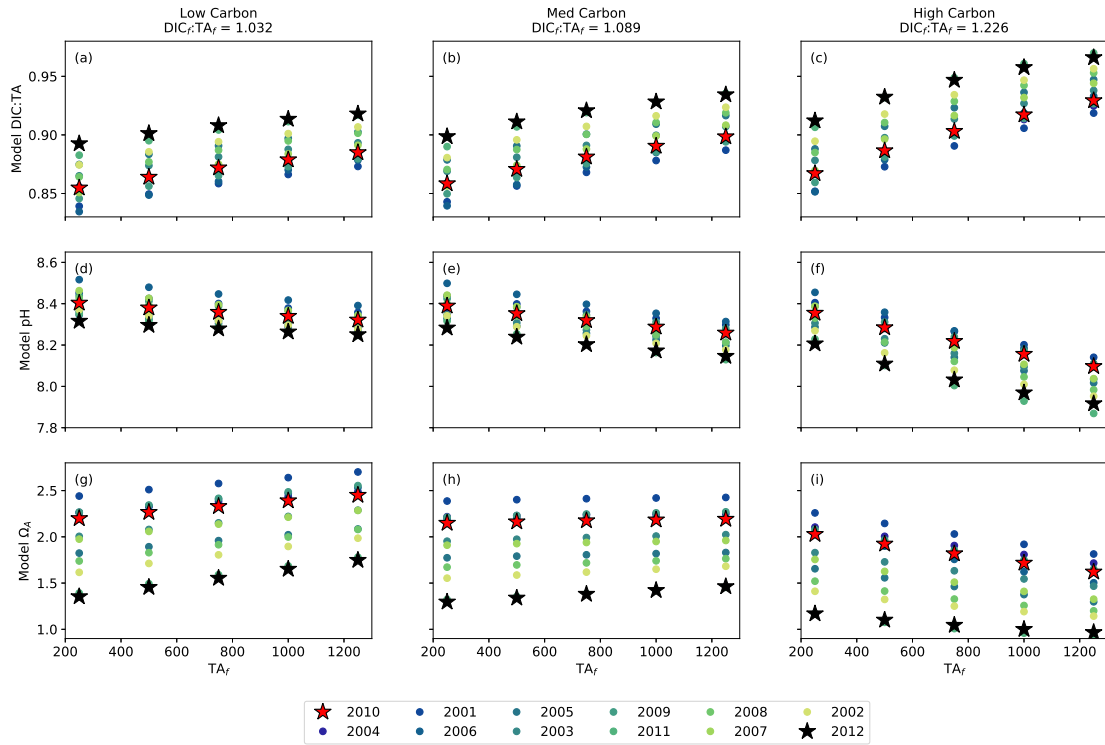


Figure 6. Salinity averaged (salinity < 20, summer) model (a-c) DIC:TA, (d-f) pH, and (g-i) Ω_A under the (left column) Low Carbon, (center column) Med Carbon, and (right column) High Carbon scenarios between all constant TA_f cases (horizontal axis) for each year in the full 12 year period (2001-2012). The salinity < 20 averages (circles) are plotted in order of increasing freshet size with the smallest (2010) and largest (2012) years highlighted as red and black stars, respectively, as in Fig. 3. Model DIC:TA (pH) generally increases (decreases) with increasing TA_f . Model Ω_A shares this trend under the High Carbon scenario but follows an opposite trend under the Low Carbon scenario. Model (a) mean, standard deviation, and min/max S calculated across the period 2001-2012, and 2001-2012 boxplots of estuarine (b, c) DIC:TA and (d, e) pH averaged over (b, d) $S < 20$ and (c, e) $S \geq 20$, and (f) summer and (g) winter estuarine $\Omega_A < 1$ duration with 6 increasing mean annual TA_f scenarios (horizontal axis, Table 2) for each of 3 pH_f scenarios (grey/white sections) moving left to right from low pH_f (high DIC_f:TA_f) to high pH_f (low DIC_f:TA_f). Model S , DIC, TA, pH and Ω_a are 0-3 m averages. Each box indicates the median, standard deviation about the mean, and 95% confidence intervals across the 12 years of runs. In (f), each box only contains runs that exhibited $\Omega_A < 1$ in summer (total labelled above each box).

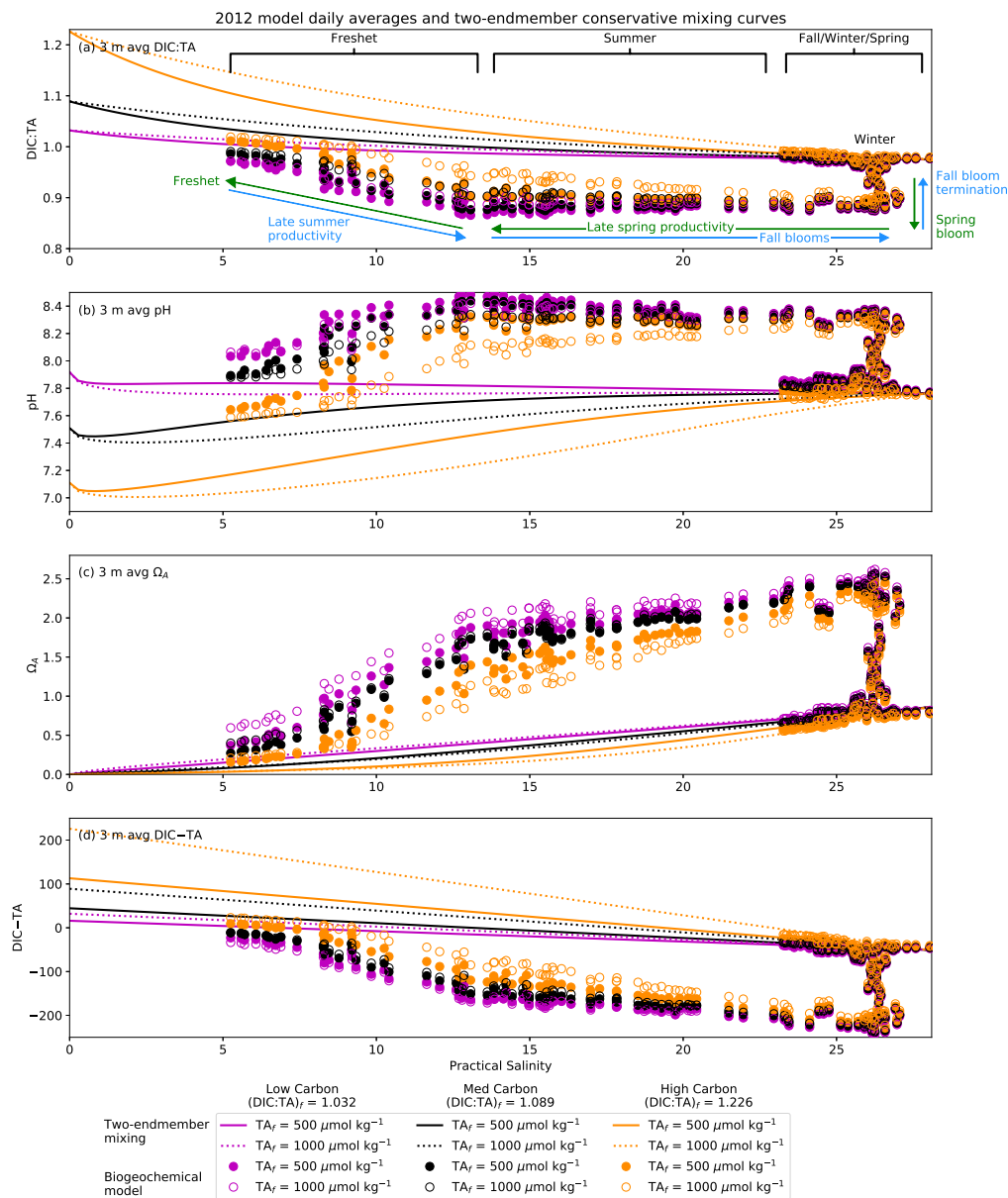


Figure 7. Daily model averages in salinity space during the largest freshet year (2012) of 3 m averaged (a) DIC:TA, (b) pH, (c) Ω_A , and (d) DIC-TA under the Low Carbon (DIC_f:TA_f = 1.032, magenta circles), Med Carbon (DIC_f:TA_f = 1.089, black circles), and High Carbon (DIC_f:TA_f = 1.226, orange circles) scenarios during 2 constant TA_f cases: TA_f = 500 $\mu\text{mol kg}^{-1}$ (filled) and TA_f = 1000 $\mu\text{mol kg}^{-1}$ (open). Theoretical conservative mixing curves between the model freshwater and seawater endmembers (Table 1) calculated using CO2SYS are also shown (lines) for the corresponding DIC_f:TA_f and TA_f cases as indicated by color and line style, respectively (see legend). All runs demonstrate significant divergence from the theoretical curves during spring and summer while converging toward the freshwater endmember at low salinity during the freshet and toward the seawater endmember at high salinity during winter, as indicated by the annotations in (a). Differences between TA_f cases in the model are otherwise similar to the conservative mixing cases, however the effect of DIC_f:TA_f in the model is reduced relative to the mixing cases. Theoretical two-endmember mixing curves of (a) DIC and TA (for pH_f = 7.7 only), (b) pH, and (c) DIC:TA for high flow (TA_f = 500 $\mu\text{eq kg}^{-1}$, solid line) and low flow (TA_f = 1350 $\mu\text{eq kg}^{-1}$, dashed line) scenarios at pH_f of 7.4 (red), 7.7 (black), and 8.0 (green). (d) Seasonal-estuarine pH differences (ΔpH) between high flow and low flow TA_f scenarios (low and high TA_f, respectively; pH_f = 7.7) for four theoretical TA_f ranges (Table ??): a tropical range similar to the Amazon (teal), a polluted range

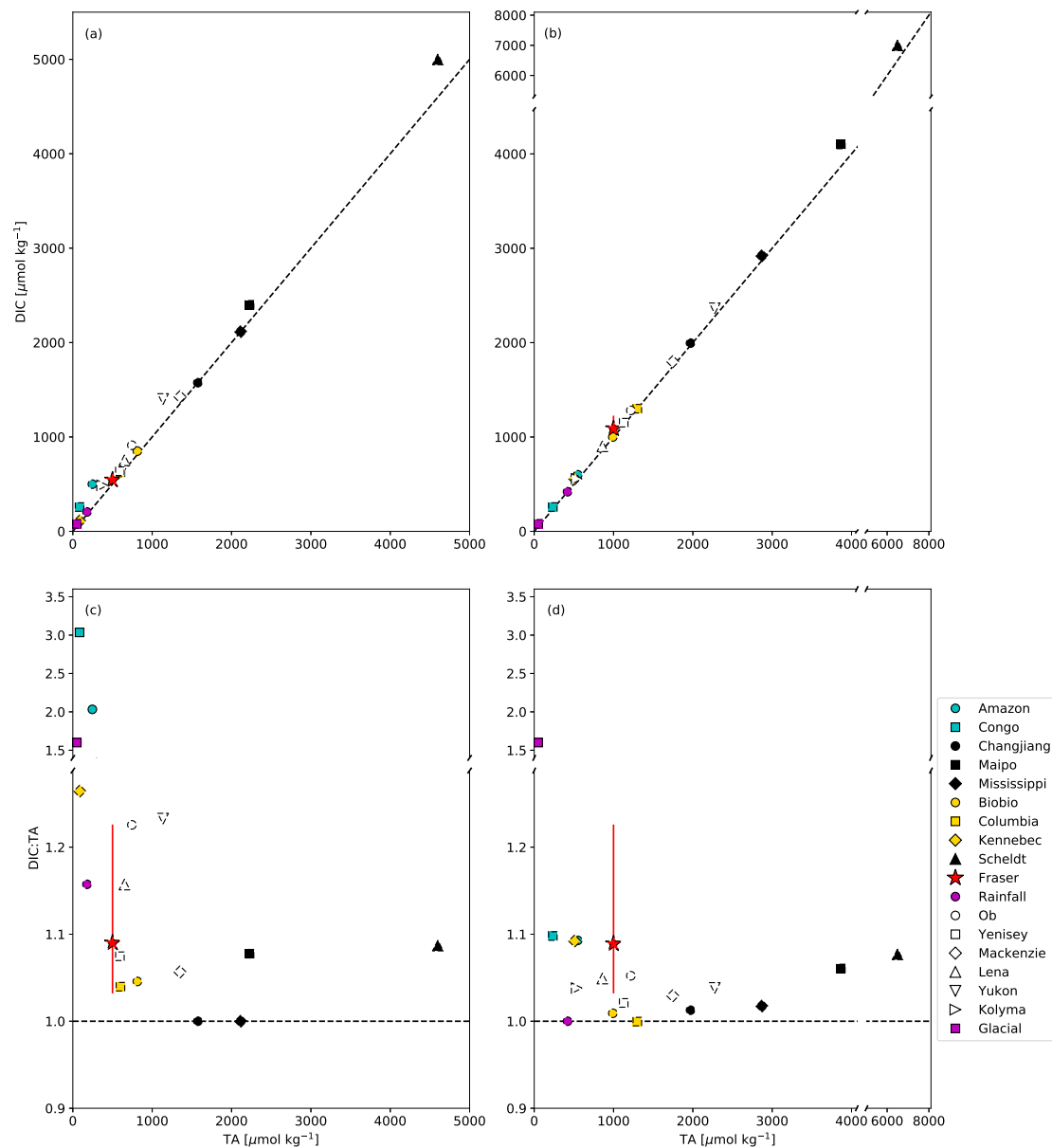


Figure 8. DIC and TA literature values for selected world rivers (Table S2) at the (a, c) low river flow (generally high TA) and (b, d) high ends of the reported ranges river flow (generally low TA). The dashed lines are the DIC:TA 1:1 lines. The legend is in order of increasing latitude. Cyan symbols represent tropical watersheds, black symbols represent urbanized/polluted watersheds, yellow symbols represent temperate watersheds, magenta symbols represent watershed type proxies, and white symbols represent Arctic watersheds. The Fraser River DIC and TA endmembers used in this study (Table 2) are shown is-emphasized as a red star with errorbars to represent the range of $\text{DIC}_f:\text{TA}_f$ scenarios. DIC data are unavailable for the Columbia River and thus calculated using reported TA and $p\text{CO}_2$ ranges. DIC and $p\text{CO}_2$ data are unavailable for the Arctic rivers and DIC is thus calculated from reported TA and pH ranges. TA data are unavailable for the Maipo and Biobio rivers and thus calculated using DIC and $p\text{CO}_2$. DIC-ranges are calculated first from $p\text{CO}_2$, next from pH when DIC observations could not be found (Table ??). TA-ranges are calculated similarly when unavailable (Maipo and Biobio rivers only). For most rivers, DIC:TA can be significantly greater than 1 (c, d) despite falling visually close to the 1:1 line (a, b). Uncertainty is not shown and not always reported.

Figure 8. Contours (light gray) of the magnitude (a) and S (b) of maximum seasonal estuarine pH differences (ΔpH) between high-low flow, two-endmember mixing curves (Fig. ??d) at $\text{pH}_f = 7.7$ as a function of mean freshwater TA ($\overline{\text{TA}}_f$) and freshwater TA range (ΔTA_f). Red lines in (a) and (b) indicate the region where $\overline{\text{TA}}_f - \Delta\text{TA}_f/2 < 0$ (i.e., negative lower ΔTA_f limit). For reference, $\overline{\text{TA}}_f - \Delta\text{TA}_f$ pairs for the Amazon (teal circle), Congo (teal square), Changjiang (black circle), Maipo (black square), Mississippi (black diamond), Biobio (yellow triangle up), Columbia (yellow triangle down), Kennebec (yellow triangle right), Scheldt (black triangle left), Fraser (red star), Rainfall Proxy (magenta circle), Glacial Proxy (magenta square), Ob (white circle), Yenisey (white square), Mackenzie (white diamond), Lena (white triangle up), Yukon (white triangle down), and Kolyma (right triangle right) Rivers (Table ??) in order of increasing latitude are also shown (a and b). All mixing curves share the same Strait of Georgia seawater endmember defined as the mean 40-m model DIC, TA, T, S, Si, and PO_4 values (Moore-Maley et al., 2016), and the same freshwater T, Si, and PO_4 defined as the mean observations near the Fraser River mouth between 2009 and 2011 (Voss et al., 2014). DIC_f and pH are calculated using CO2SYS (Lewis and Wallace, 1998) and full S -range K_1 and K_2 dissociation constants (Millero, 2010).

Table 1. Model freshwater and seawater endmembers used to prescribe river fluxes and values at the 40 m boundary.

Endmember	Salinity [PSS-78]	Temperature [°C]	DIC [$\mu\text{mol kg}^{-1}$]	TA [$\mu\text{mol kg}^{-1}$]	Dissolved phosphorus ^a [$\mu\text{mol kg}^{-1}$]	Dissolved silica [$\mu\text{mol kg}^{-1}$]
Freshwater	0	10.9 ^b	see Table 2	see Table 2	0.8	80.0
Seawater ^c	29.6	9.1	2020.0	2050.4	1.9	78.2

^a Approximated from nitrate using the Redfield Ratio

^b Midpoint of the model freshwater temperature range (2.5–19.3°C)

^c Values presented are averages as seawater endmembers, except for nitrate and dissolved silica, are variable in the model

Table 2. Biogeochemical model freshwater endmember cases run for each year in the 2001-2012 year range.

ID	Name	(DIC:TA) _f	pH _f ^(a)	TA _f (μeq kg ⁻¹)	DIC _f (μeq kg ⁻¹)	DIC _f - TA _f (μeq kg ⁻¹)
LC1				250	258	8
LC2				500	516	16
LC3	Low	1.032	7.8-8.0	750	774	24
LC4	Carbon			1000	1032	32
LC5				1250	1290	40
LCV ^(b)				580-1015 ^c	599-1047	19-32
MC1						250
MC2				500	544	44
MC3	Med	1.089	7.4-7.6	750	817	67
MC4	Carbon			1000	1089	89
MC5				1250	1361	111
MCV ^(b)				580-1015 ^c	632-1105	52-90
HC1						250
HC2				500	613	113
HC3	High	1.226	7.0-7.2	750	920	170
HC4	Carbon			1000	1226	226
HC5				1250	1532	282
HCV ^(b)				580-1015 ^c	711-1244	131-229

^apH_f range is across the model freshwater temperature range of 2.5-19.3°C

^bVariable TA_f is given in Equation 1

^cVariable TA_f parameter ranges are the 1st and 99th percentiles across the 12 year (2001-2012) dQ_{filt}/dt daily record

Table 2. Datasets used to assess the range and variability of freshwater TA and pH near the Fraser River estuary.

Dataset	Locations(s) ^a	Years	Frequency	Qty	Units ^b	Method
Endmember TA ^c	See de Mora (1983)	1978—1979	seasonal	TA	mmol L ⁻¹	Anderson and Robinson (1946)
	See Ianson et al. (2016)	2010—2012	seasonal	TA	$\mu\text{mol kg}^{-1}$	Dickson et al. (2007)
Buoy pH ^d	Main Arm	2008—2013	hourly	pH	NIST units ^e	Ethier and Bedard (2007)
Hope TA ^f	Hope	1979—1999	semi-monthly	TA	mg CaCO ₃ L ⁻¹	Environment Canada (2006)
Rivermouth TA ^f	North and Main Arm	2004—2009	semi-monthly	TA	mg CaCO ₃ L ⁻¹	Environment Canada (2006)

^aSee Fig. 1.

^bTA converted to $\mu\text{mol kg}^{-1}$ for use in the present study (Sect. ??).

^cde Mora (1983); Ianson et al. (2016).

^dECCC Fraser River Water Quality Buoy (<http://aquatic.pyr.ec.gc.ca/RealTimeBuoys/fraserRiverChart.aspx>).

^eNational Institute of Standards and Technology scale.

^fEnvironment and Climate Change Canada (ECCC, <http://aquatic.pyr.ec.gc.ca/webdataonlinenational>).

Table 2. SoG- $TA_{\mathcal{F}}$ scenarios based on fits between Fraser River and SoG- TA data and the estimated (Pawlowicz et al., 2007) Fraser River discharge, Q , near the delta (Fig. ??).

	Scenario	$TA_{\mathcal{F}}(\mu\text{eq kg}^{-1})^a$	Q limit ^b
1	Minimum- $TA_{\mathcal{F}}$	500	
2	Endmember-Fit	$1116 - 165.3Q_n + 12.5Q_n^2$	$< 11,000$
3	Rivermouth-Fit	$935 - 18.9Q_n$	
4	Mean- $TA_{\mathcal{F}}$	900	
5	Hope-Fit	$1167Q_n^{-0.157}$	> 400
6	Maximum- $TA_{\mathcal{F}}$	1350	

^a $Q_n = Q/1000 \text{ m}^3 \text{ s}^{-1}$

^bDesignates the range of Q ($\text{m}^3 \text{ s}^{-1}$) where the scenario is valid (closest valid point used beyond this range).